C1 neurons mediate a stress-induced anti-inflammatory reflex in mice

Chikara Abe[1,3,#], **Tsuyoshi Inoue**[2,#], **Mabel A. Inglis**[1], **Kenneth E. Viar**[1], **Liping Huang**[2], **Hong Ye**[2], **Diane. L. Rosin**[1], **Ruth L. Stornetta**[1], **Mark D. Okusa**[2], and **Patrice G Guyenet**[1,*]

[1]Department of Pharmacology, University of Virginia, Charlottesville, Virginia

[2]Department of Medicine, Division of Nephrology and Center for Immunity, Inflammation, and Regenerative Medicine, University of Virginia, Charlottesville, Virginia

Abstract

C1 neurons (C1), located in the medulla oblongata, mediate adaptive autonomic responses to physical stressors (e.g. hypotension, hemorrhage, lipopolysaccharide). We describe here a powerful effect of restraint stress mediated by C1: protection against renal ischemia-reperfusion injury (IRI).

Restraint stress or optogenetic C1 stimulation (10 min) protected mice from IRI. The protection was reproduced by injecting splenic T-cells pre-incubated with noradrenaline or splenocytes harvested from stressed mice. Stress-induced IRI protection was absent in *α7nAChR*$^{-/-}$ mice and greatly reduced by destroying or transiently inhibiting C1. The protection conferred by C1 stimulation was eliminated by splenectomy, ganglionic blocker administration, or β$_2$-adrenergic receptor blockade. Although C1 stimulation elevated plasma corticosterone and increased both vagal and sympathetic nerve activity, C1-mediated IRI protection persisted after subdiaphragmatic vagotomy or corticosterone receptor blockade.

In conclusion, acute stress attenuates IRI by activating a cholinergic, predominantly sympathetic, anti-inflammatory pathway. C1 neurons are necessary and sufficient to mediate this effect.

*Corresponding Author: Patrice G. Guyenet, PhD, 1300 Jefferson Park Avenue, P.O. Box 800735, Charlottesville, VA 22908-0735. Tel: 434 924-9974. Fax: 434 982-3878. pgg@virginia.edu.
[3]Current address: Department of Physiology, Gifu University Graduate School of Medicine, Gifu, Japan
[#]These authors contributed equally to this work.

Accession codes:

Introduction

Activation of the immune system and leukocyte infiltration lead to tissue and organ injury in both acute (ischemia-reperfusion injury (IRI))[1] and chronic (rheumatoid arthritis) conditions[2]. The cholinergic anti-inflammatory pathway (CAP) has been defined as the efferent arm of a vagal reflex that limits the duration and intensity of the inflammatory response[2–6]. The CAP is elicited by electrical stimulation of the vagus nerve or by non-invasive ultrasound treatment[7], procedures that have beneficial effects in a number of inflammatory models including renal IRI[2, 8]. The CAP is mediated by the spleen and its noradrenergic innervation[9]. The intrasplenic pathway includes activation of β_2 adrenergic receptors expressed by choline acetyl-transferase+ (ChAT+) splenic memory T cells (CD4+CD44highCD62Llow)[10, 11], acetylcholine (ACh) release by these leukocytes, and activation of α7 nicotinic receptors (α7nAChRs) on adjacent macrophages leading to reduced production of pro-inflammatory cytokines[12]. A parallel sympathetic anti-inflammatory reflex, also converging on the spleen, contributes to the immunosuppressive effect of spinal injury[13] or anesthesia[14].

Of note, stimulating the central or the distal end of a divided cervical vagus nerve provides equal protection against renal IRI in mice[8]. Moreover, the renal protection conferred by stimulating the central end of the vagus nerve persists even if the stimulus is delivered while the contralateral vagus nerve is blocked[8]. Altogether, this type of evidence suggests that anti-inflammatory reflexes are not exclusively vago-vagal and that, in some cases, the neural component of the CAP may rely on a canonical sympathetic route (splenic noradrenergic neurons activated by sympathetic cholinergic preganglionic neurons residing in the spinal cord)[15].

Inflammatory reflexes are almost certainly regulated by the CNS because the CAP is activated by intracerebral administration of drugs[2, 16, 17] and brain death unleashes peripheral inflammation[18]. Identifying and ultimately stimulating the CNS pathways that control the CAP could be of benefit in the management of chronic inflammatory diseases, spinal injury and organ transplantation[2, 13, 18–20].

The autonomic nervous system, notably its sympathetic division is mobilized by physical and psychological stressors[21–23]. A subset of these autonomic responses (especially cardiovascular) is mediated or facilitated by C1 neurons, a group of glutamatergic/catecholaminergic/peptidergic neurons that reside in the medullary reticular formation[21–23]. Acute stress also mobilizes the immune system, as evidenced by rapid reductions in thymus and spleen volume and increased leukocyte flux in blood[24]. Though better known for their role in controlling sympathetic efferents, C1 neurons also innervate the dorsal motor nucleus of the vagus and the paraventricular nucleus of the hypothalamus[25, 26]. In addition, subsets of C1 cells are strongly activated by circulating interleukin-1 and lipopolysaccharide as well as footshock[21]. Therefore, we asked whether acute stress reduces tissue injury by activating the CAP and we tested whether C1 neurons are a critical node for central regulation of this neuroimmune anti-inflammatory reflex.

Results

Restraint stress protects the kidneys from IRI

Most experiments were conducted in dopamine β-hydroxylase$^{Cre/0}$ (hereafter DBH-cre) mice. We first examined whether a brief period of restraint stress provides protection in an IRI model and whether the CAP contributes to the protective action. We chose to examine renal IRI, evoked by 26 min of ischemia (bilateral clamping of the renal arteries and veins) and followed by 24 hours of tissue reperfusion, because renal damage can be precisely quantified by three complementary measures: plasma creatinine (a measure of kidney function), kidney *Kim-1* transcripts (a.k.a. *Havcr1*, a biomarker of renal proximal tubule injury), and histological examination of renal tubular necrosis[7, 8, 27].

A 10 min period of physical restraint provided strong protection from kidney injury evoked by renal ischemia-reperfusion (IR) 24 hours later (Figure 1a), as shown by lower plasma creatinine (0.44 ± 0.18 vs. 1.38 ± 0.08 mg/dL; n = 6/group) (Figure 1b), reduced *Kim-1/ Gapdh* mRNA ratio (Figure 1c) and lesser degree of tubular necrosis (Figure 1d; Suppl. Figure 1) compared to unstressed mice. Of note, stress did not totally protect the mice against IR injury; all three markers of injury were significantly higher in stressed mice subjected to renal IR than in DBH-cre mice subjected neither to stress nor renal IR (Figure 1b–d).

The CAP requires α7nAChRs that are expressed by splenic macrophages and, possibly, by the noradrenergic innervation of the spleen[2, 15, 28]. As an initial test of whether restraint stress protects against renal IRI by activating this pathway, we examined whether restraint protects the kidneys in *α7nAChR$^{−/−}$* (α7KO) mice. Restraint stress did not ameliorate the renal IRI in these mice but it effectively protected genetically matched controls (α7WT), as evidenced by a greatly reduced plasma creatinine level 24 hrs after renal IR (Figure 1e).

Seeking further evidence that restraint stress protects mice from kidney IRI by activating the CAP, we first examined whether splenocytes harvested from stressed C57BL/6 mice confer protection against renal IRI to unstressed mice of the same strain (Figure 2a). Injection of splenocytes protected unstressed recipient mice from renal IRI in a dose-dependent fashion regardless of the donor but protection required significantly fewer cells when the splenocytes originated from stressed mice (Figure 2b). Activation of splenic T-lymphocytes by noradrenaline is a critical stage of the CAP. We therefore tested whether administration of CD4 T-lymphocytes harvested from the spleen of unstressed C57B/6 mice and incubated with noradrenaline *in vitro* would protect unstressed mice from renal IRI (Figure 2c). This was indeed the case (Figure 2d).

In brief, a short period of physical restraint (10 min) protects the kidneys from IRI inflicted 24 hours later. The same degree of protection was observed in two strains of mice (DBH-cre and α7WT). The protection conferred by stress was absent in α7KO mice; it was transferable to naive mice by injecting splenocytes harvested from stressed mice or by injecting splenic CD4 T-cells harvested from naïve mice and exposed to noradrenaline *in vitro*. These results suggest that restraint stress, like vagus nerve stimulation and non-invasive ultrasound[8, 27], protects mice from renal IRI by activating the CAP.

Selective optogenetic stimulation of C1 neurons protects the kidneys from IRI

The C1 neurons are activated by physical stresses such as hypoxia, hemorrhage, hypoglycemia and infection[23] and, as a group, the C1 neurons heavily innervate both sympathetic and vagal preganglionic neurons as well as the paraventricular nucleus of the hypothalamus[29]. If activated, each of these CNS output pathways could potentially elicit anti-inflammatory effects. Accordingly we first asked whether selective stimulation of C1 neurons also protects mice against renal IRI. Five to six weeks after injecting a FLEX (flip-excision) ChR2-mCherry vector (AAV2–DIO–EF1α–ChR2(H134R)–mCherry, hereafter AAV2–ChR2–mCherry) into the left rostral ventrolateral medulla oblongata (RVLM) of DBH-cre mice, Cre-mediated recombination and channelrhodopsin2 (ChR2) expression was confined to tyrosine hydroxylase-immunoreactive (TH$^+$) neurons located within the ventrolateral medulla 6.1–7.2 mm caudal to bregma (Figure 3b; Suppl. Figure 2a). In mice, most (>95%) TH$^+$ neurons located within this region of the medulla oblongata contain phenylethanolamine N-methyl transferase (PNMT) transcripts[30], therefore most of the ChR2$^+$ neurons were, by definition, C1 adrenergic cells. Five to six weeks after injection of the control vector into the left medulla oblongata (AAV2–DIO–EF1α–mCherry, abbreviated DIO-mCherry), mCherry immunoreactivity was also confined to TH$^+$ neurons located in the RVLM (results not shown).

Unilateral optogenetic stimulation of C1 neurons was performed in unanesthetized mice 24 hours before renal IR (Figure 3a; optrode placements illustrated in Figure 3b and Suppl. Figure 2b). In anesthetized mice each light pulse evokes a single action potential in C1 neurons[26]. The stimulation parameters (5 Hz, 10 ms pulses) were selected to produce a small submaximal respiratory stimulation (Suppl. Figure 2c–f; Suppl. Table 1). C1 stimulation was maintained for 10 min in order to match the duration of the restraint stress. C1 cell stimulation reduced behavioral activity and locomotion while eliciting a regular, slightly increased, breathing rate (Suppl. Figure 3). These effects ended upon cessation of the stimulus (Suppl. Figure 3). Respiratory stimulation and reduced behavioral activity were caused by C1 cell activation and not by the light itself because they were undetectable in the 6 DBH-cre mice that had received injections of control vector (DIO-mCherry; results not shown).

Plasma creatinine, *Kim-1/Gapdh* mRNA ratio and tubular necrosis were low in mice subjected to sham surgery and, as expected for renal IRI, these parameters were elevated 24 hours after renal IR (Figure 3c–e; Suppl. Figure 4). C1 cell stimulation greatly reduced all three indices of renal pathology elicited by IR (Figure 3c–e; Suppl. Figure 4). By contrast, blue laser illumination of the ventrolateral medulla of DBH-cre mice that had received the control vector AAV2-mCherry had no protective effect (Figure 3c–e; Suppl. Figure 4). In short, mild, selective, optogenetic stimulation of C1 neurons produced behavioral quiescence, increased breathing slightly and protected against renal IRI inflicted 24 hrs later.

Renal IRI protection by restraint stress requires C1 neurons

Next, we tested whether the beneficial effect of restraint stress would be attenuated in mice in which the C1 cells were inhibited during the stress period. We transduced C1 cells to express Gi-coupled DREADD (designer receptor exclusively activated by designer drug[31])

by injecting AAV2–DIO–hSyn–hm4D(Gi)–mCherry bilaterally into the RVLM of DBH-cre mice. When activated, this receptor inhibits neurons that express inwardly-rectifying potassium channels, which is the case of C1 cells[32]. mCherry immunoreactivity, indicating the presence of DREADDs, was detected predominantly in catecholaminergic neurons (75.3 ± 2.2% of mCherry$^+$ neurons were also TH$^+$) and 43.2±4.2% of C1 neurons (RVLM TH$^+$ neurons) contained mCherry (Figure 4a, b). The lower selectivity of the DREADD-expressing AAV2 for catecholaminergic neurons relative to the other FLEX vectors (75% vs. >95% TH$^+$ neurons) presumably results from a difference in promoter (synapsin vs. EF1α). Administration of the DREADD agonist, clozapine N-oxide, 15 min before restraint significantly reduced the protective effect of stress, unlike injection of vehicle (Figure 4e).

We also examined whether the protective effect of restraint stress would be attenuated if C1 cells were selectively destroyed. To that end we injected AAV2–DIO–taCasp3–TEVp, a FLEX caspase-expressing AAV2 vector, bilaterally into the RVLM of DBH-cre mice[33]. Within a week, this procedure eliminated most TH$^+$ neurons located within the brain region of interest (Figure 4c, d). All other (nor)adrenergic cell groups (dorsal vagal complex, dorsal medulla, locus coeruleus) appeared intact. Non-specific tissue damage was not detected at the site of vector injection and the cholinergic neurons that are co-mingled with C1 were intact (Figure 4c). These lesions reduced dramatically the protective effect of restraint stress against renal IRI (Figure 4e).

Thus, acute DREADD-mediated inhibition or caspase-mediated destruction of C1 neurons eliminates the protective effect of restraint stress against renal IRI, implying an obligatory role for these brainstem cells in the stress-evoked anti-inflammatory reflex.

Corticosterone release does not account for the protective effect of restraint stress or C1 cell stimulation against renal IRI

Stress activates corticosterone synthesis and release (e.g.[34]). A subset of C1 cells innervate the hypothalamic paraventricular nucleus and likely contribute to the activation of the CRF/ACTH/corticosterone cascade[35]. Corticosterone has anti-inflammatory effects that could conceivably explain the reduced renal damage following restraint stress and/or C1 cell stimulation. Both restraint stress (10 min) and optogenetic activation of C1 cells (10 min, 5 Hz) increased plasma corticosterone in unanesthetized DBH-cre mice, although the hormonal rise elicited by C1 stimulation was smaller than that elicited by restraint (Figure 5a, b). The plasma corticosterone surge elicited by C1 cell stimulation was not caused by handling the animals nor by the light itself because brainstem illumination did not change the corticosterone level in mice that had received injections of control vector (AAV2-mCherry) (Figure 5b).

In order to test whether corticosterone mediates the renal IRI protection elicited by C1 cell stimulation, we administered the corticosterone antagonist mifepristone to DBH-cre mice prior to stimulating C1 cells optogenetically. Mifepristone did not reduce the renal protective effect, suggesting that the beneficial effect of C1 cell stimulation against renal IRI is not mediated by the rise in plasma corticosterone (Figure 5c).

C1 neuron stimulation activates the autonomic nervous system

As shown before[26], optogenetic stimulation of C1 cells in anesthetized DBH-cre mice (10 ms pulses, 5–20 Hz, 10 s trains) produced a robust and sustained frequency-dependent increase in multi-fiber efferent vagus nerve activity on the ipsilateral side (Figure 6a). We add here that contralateral efferent vagus nerve activity was also increased by stimulating C1 cells at 5 Hz or above, albeit to a lesser degree (Figure 6b). These results agree with the existence of a dominantly ipsilateral monosynaptic excitatory connection between C1 cells and the dorsal motor nucleus of the vagus[25]. For technical reasons, sympathetic nerve activity was recorded from a renal nerve rather than a splenic nerve. Low frequency stimulation of C1 cells (1 Hz) evoked a robust phasic response in the renal sympathetic nerve (onset latency: 59 ± 4.7 ms; peak latency: 102.8 ± 11.7 ms) (Figure 6c). Trains of stimuli delivered at 5–20 Hz also increased mean renal sympathetic nerve activity (Dummy vs. 20 Hz: $p = 0.005$; 5 Hz vs. 20 Hz: $p = 0.0164$; Figure 6d).

These observations agree with and extend prior evidence that C1 neurons are excitatory and directly innervate both sympathetic and vagal parasympathetic preganglionic neurons[26].

Contribution of the spleen and the autonomic nervous system to the protective effect of C1 cell stimulation against renal IRI

In order to test whether C1 cell activation protects mice against renal IRI by activating the autonomic nervous system, we administered the ganglionic blocker hexamethonium 30 min before stimulating the C1 neurons optogenetically (Figure 7a). These experiments were performed in DBH-cre mice that had received unilateral injections of AAV2-ChR2-mCherry five weeks prior. Hexamethonium greatly attenuated the renal protection elicited by C1 neuron stimulation (Figure 7a); thus activation of vagal and/or sympathetic efferents is required for C1 neurons to protect against renal IRI.

The spleen is a critical component of the CAP[3] and electrical stimulation of the vagus nerve protects the kidneys from IRI only if the spleen is intact[8]. Splenectomy, performed 7 days before stimulating C1 cells, also eliminated the protective effect of C1 cell stimulation against renal IRI (Figure 7b). This result, the fact that C1 cell stimulation increases vagal and sympathetic efferent activity, and the efficacy of hexamethonium suggested that C1 cell stimulation, like restraint stress, protected the kidneys by activating the CAP[3]. The CAP requires activation of β_2-adrenergic receptors expressed by splenic T cells[11]. Accordingly, we tested whether β_2-adrenergic receptor blockade would prevent the protective effect of C1 cell stimulation against renal IRI (Figure 7a). Butoxamine, a β_2-selective antagonist that blocks the CAP in mice[11] eliminated the protective effect of C1 cell stimulation (Figure 7a). We also tested labetalol, a non-selective $\beta_1/\beta_2/\alpha_1$ adrenergic blocker in humans. However, this agent was ineffective (results not illustrated), perhaps reflecting weak blockade of β_2-receptors in mice or some consequence of its additional actions on β_1- and/or α_1-receptors in the CNS or elsewhere.

Both vagal and sympathetic preganglionic neurons appear capable of triggering the CAP[3, 14]. In order to identify which division of the autonomic nervous system mediates the renal IRI protection elicited by C1 cell stimulation we performed subdiaphragmatic vagal

denervations (Figure 7c). First, we tested the efficacy of the surgical procedure by injecting the retrogradely transported dye Fluoro-Gold (FG) intraperitoneally. As expected, in sham-operated mice, the dye was abundantly present in the dorsal motor nucleus of the vagus (Suppl. Figure 5). By contrast, FG was absent from this nucleus in mice in which vagus nerve branches had been cut immediately below the diaphragm (n = 3 in each group; Suppl. Figure 5). We then determined whether the renal protection produced by C1 cell stimulation was attenuated in mice with subdiaphragmatic vagal denervation; it was not (6 mice per group; Figure 7c). Thus, the subdiaphragmatic vagus nerve is not required for C1 cell stimulation to activate the CAP and protect the kidneys from IRI. Since the protection is greatly reduced by ganglionic blockade but unaffected by mifepristone, the C1 neurons most likely activate the CAP via a sympathetic route.

Restraint stress and C1 cell stimulation produce opposite effects on AP and HR

Given that restraint stress and C1 cell stimulation are equally effective at protecting the kidneys against IRI, we wondered whether these two stimuli produce similar hemodynamic effects and whether the latter could conceivably account for protection. Telemetric probes were implanted to record pulsatile arterial pressure (AP) from a carotid artery and the heart rate (HR) was ultimately derived from these recordings. As expected, restraint stress elevated AP (from 97.4 ± 3.1 to 112.2 ± 1 mmHg) and HR (from 423.4 ± 17.6 to 595.6 ± 18.2 mmHg; n = 4; Figure 8 a–c). These changes persisted for at least another 10 min after the mice were returned to their home cage. By contrast, C1 cell stimulation at 5 Hz for 10 min lowered AP (from 110.1 ± 2 to 92 ± 2.5 mmHg) and HR (from 593.5 ± 22.6 to 461.3 ± 24 mmHg; n = 4; Figure 8d–f) and these parameters returned to control less than a minute after the end of the stimulus (Figure 8d–f).

In short, C1 cell stimulation produced a cardiovascular response usually associated with freezing behavior (reduced locomotion, decreased HR) whereas restraint stress produced a pattern more reminiscent of fight or flight behavior (increased HR and BP)[36]. Both responses are associated with a reduction in renal and splanchnic blood flow[36], suggesting that C1 cell stimulation and restraint stress could perhaps have protected the kidneys against IRI via ischemic preconditioning[37]. In order to test the plausibility of such interpretation we determined whether 10 min of C1 cell stimulation in a conscious mouse produces a measurable increase in the renal level of hypoxia inducible factor *1a* (*Hif1a*) transcripts. Renal *Hif1a/Gapdh* mRNA ratio was unchanged by C1 cell stimulation but subjecting the kidneys of anesthetized mice to a short period of ischemia (10 min), which does not produce any detectable renal damage, increased this ratio significantly (Suppl. Figure 6). In short, we found no evidence that C1 cell stimulation for 10 min produces renal ischemia.

Discussion

This study demonstrates that acute restraint stress protects the kidneys from IRI and that C1 neurons are necessary and sufficient for this effect to occur. Restraint stress and C1 cell stimulation produced an equivalent degree of protection against renal IRI by three different measures: plasma creatinine, *Kim-1* transcripts and histological analysis of renal tubular damage. Like the protection against renal IRI elicited by ultrasound or vagal efferent

stimulation[8, 27], the beneficial effect of restraint stress or C1 stimulation was mediated by the splenic CAP. The protection elicited by C1 neuron stimulation, though mediated by the autonomic nervous system, did not require the subdiaphragmatic vagus nerve.

We conclude that C1 neurons could be a nodal point of the neuro-immune reflex mediated via the CAP and suggest that this anti-inflammatory pathway can be activated predominantly via a sympathetic rather than vagal preganglionic efferent pathway.

Mechanism of injury protection by stress and the C1 neurons

C1 cell stimulation elevated plasma corticosterone, albeit to a lesser extent than restraint. Yet, this hormone did not contribute detectably to the protection from renal IRI because the protection was unaffected by the corticosteroid receptor antagonist mefipristone. While both restraint stress and C1 cell stimulation activate sympathetic nerve activity and probably reduce renal and splanchnic blood flow[36], the degree of flow reduction is unlikely to be sufficient to trigger ischemic or remote ischemic preconditioning. Supporting this view, renal $Hif1a$ mRNA level increases after mild renal ischemia (10 min, present results) and remote ischemic preconditioning[37] but we detected no such increase after C1 cell stimulation.

The autonomic nervous system and the spleen were clearly implicated in the injury protection elicited by restraint stress or C1 cell stimulation because splenectomy, ganglionic blockade or administration of a selective β_2 adrenergic receptor antagonist eliminated the protection. In addition, renal IRI protection could be conferred to naïve mice by transferring splenocytes harvested from stressed mice or by injecting noradrenaline-treated CD4 splenic lymphocytes. Finally, stress had no beneficial effect in $\alpha 7nAChR^{-/-}$ mice. The latter evidence does not implicate specifically the α7nAChRs that are located on splenic macrophages since this receptor type is also expressed within the CNS and by sympathetic efferent neurons but it is consistent with the notion that the renal protection is mediated by the CAP as originally defined[2, 3, 11]. The renal protection elicited by stress or C1 cell stimulation seems to operate via the same peripheral mechanism as that produced by peripheral vagus nerve stimulation or non-invasive ultrasound[8, 27]. In each case, protection was absent in $\alpha 7nAChR^{-/-}$ mice, it was eliminated by splenectomy and it was transferrable to naïve mice by administration of splenic T-lymphocytes harvested from animals previously subjected to the protective stimulus. In the case of ultrasound, no protection was observed in mice deficient in functional T and B lymphocytes ($Rag1^{-/-}$) and protection could be reinstated by administering wild-type CD4+ T cells intravenously unless the spleen was excised[27]. We have not yet tested whether stress or C1 stimulation fails to protect the kidneys from IRI in $Rag1^{-/-}$ mice but this outcome is likely.

The present study does not further clarify how the kidneys are ultimately protected from injury after the spleen is activated. In the case of vagus nerve stimulation, the protection correlates with a reduction in renal granulocyte infiltration, a decrease of the concentration of inflammatory cytokines in the plasma and the renal parenchyma and a possible M1 to M2 phenotypic shift of circulating macrophages[8].

Vagal vs. sympathetic routes of activation of the CAP

The CAP requires the activation of the splenic nerve[2, 11] which is presumed to consist almost entirely of noradrenergic axons with cell bodies located in the suprarenal and celiac ganglia[9, 38]. Under anesthesia, most active splenic nerve fibers are reportedly under arterial baroreceptor control; these efferent fibers presumably innervate the spleen vasculature and derive their ongoing activity from the brainstem via sympathetic preganglionic neurons[39]. The white pulp of the spleen, especially the central region that harbors the T-lymphocytes also receives a dense noradrenergic innervation, which likely mediates the CAP. There is mounting albeit incomplete evidence that the noradrenergic neurons that innervate the spleen receive input from both vagal and sympathetic preganglionic neurons[2, 14]. Supporting the vagal efferent hypothesis, renal IRI protection and other CAP-related effects are elicited by stimulating the peripheral end of a cut vagus nerve[8, 40]. Such results implicate vagal efferent neurons or, less likely, an axon reflex. Anatomical connections between the dorsal motor nucleus of the vagus and the spleen have been detected, although not by all investigators[41,42,38] and anatomical contacts between vagal preganglionic neurons and prevertebral ganglionic (presumably noradrenergic) neurons have also been described[43] although evidence that these ganglionic neurons innervate the spleen is yet to be produced[38].

In the present study, the renal protection produced by C1 cell stimulation was greatly attenuated by ganglionic blockade but was unaffected by subdiaphragmatic vagal denervation. This evidence does not rule out the possibility that stress or C1 stimulation could also activate the catecholaminergic neurons that regulate splenic T cells via a vagal preganglionic route, especially since C1 stimulation activates vagal efferents. However, the present evidence indicates that activation of sympathetic efferents was sufficient to activate the CAP and elicit the protection. A similar sympathetic mechanism contributes to the immunosuppressive effects of anesthesia or spinal transection[13, 15], two conditions under which sympathetic tone can be extremely elevated.

C1 cells: beyond cardiovascular homeostasis

C1 neurons are glutamatergic and catecholaminergic and differentially express several neuropeptides (e.g. neuropeptideY, substance P, enkephalin)[23]. Subsets of these neurons are believed to operate as a switchboard for eliciting behaviorally appropriate patterns of autonomic responses[23, 44, 45]. Only a third of the C1 neurons innervate sympathetic preganglionic neurons[46]. These particular C1 neurons contribute to blood pressure and glucose homeostasis via sympathetic reflexes that are predominantly organized at lower levels of the neuraxis[22, 23, 47]. In addition to their homeostatic function, C1 cells also have an allostatic role (arousal from sleep, freezing behavior, cardiorespiratory adjustments) that is revealed when they are selectively activated ([45], present results). One interpretation of the present study is that a subset of C1 cells, currently unidentified, regulates the immune system during psychological and possibly other forms of stress[24]. The predominantly sympathetic route of activation of the anti-inflammatory splenic mechanism elicited by C1 cell stimulation suggests that this subset of C1 cells could be bulbospinal. However, this argument is not compelling. Bulbospinal and hypothalamus-projecting C1 cells also target a common set of CNS structures that are implicated in autonomic regulations (dorsal vagal complex, parabrachial nuclei, periaqueductal gray matter, locus coeruleus and other

noradrenergic neurons)[29, 30]; activation of any one of these structures could ultimately increase sympathetic efferent activity and activate the CAP via descending pathways other than the bulbospinal C1 cells[30]. The C1 cells belong to the lower brainstem reticular core and respond to a wide variety of stimuli; for example, they are excited by restraint stress and by somatic as well as visceral, notably vagal, afferents[23, 48]. This vagal sensory input could explain why activating the central end of a divided vagal nerve also protects the kidneys from IRI[8]. This broad set of inputs combined with the ability of the C1 cells to activate parasympathetic and sympathetic efferents[29] may explain why the CAP can be activated by triggers as diverse as stimulation of vagal afferents or efferents, stimulation of the auricular nerve[49], stress and electro-acupuncture[50]. In other words, CAP activation may be one of a constellation of stereotyped effects (arousal, cardiorespiratory stimulation) elicited or facilitated by the C1 cells in response to internal or external "danger" signals. Intense or artificially synchronized afferent fiber activity, such as produced by repetitive electrical stimulation of the vagal nerve or subsets of somatic afferents (acupuncture), may be such a trigger.

In conclusion, C1 cells mediate the protective effect of stress against renal IRI by activating the CAP. In this particular case the CAP seems to be activated via a sympathetic rather than vagal route. This study also provides proof of principle that localized brain stimulation can produce beneficial anti-inflammatory effects.

On-line Methods

Animals

Animal use was in accordance with the NIH Guide for the Care and Use of Laboratory Animals and was approved by the University of Virginia Animal Care and Use Committee. $D\beta H^{Cre/0}$ mice were obtained from the Mutant Mouse Regional Resource Center at the University of California, Davis, CA [Tg(DβH-cre)KH212Gsat/Mmcd; stock no. 032081-UCD]. $D\beta H^{Cre/0}$ mice were maintained as hemizygous (Cre/0) on a C57BL/6J background. A total of 182 $D\beta H^{Cre/0}$ male mice (DBH-cre), aged between 10 and 14 weeks, were used for these experiments. $Chrna7^{-/-}$ (referred to as α7KO) mice (B6.129S7-Chrna7tm1Bay/J) were obtained from Jackson Laboratories, and WT ($Chrna7^{+/+}$) progeny were used as controls in this experiment (n = 12 in α7WT and n = 10 in α7KO). For the adoptive transfer (n = 56) and Fluoro-Gold (FG, n = 6) experiments, we used WT NCI C57BL/6 mice that were purchased from Charles River Laboratories.

Viral vectors

AAV–DIO–EF1α–Channelrhodopsin2(H134R)–mCherry serotype 2 (AAV2–ChR2–mCherry), AAV–DIO–EF1α–mCherry serotype 2 (AAV2–mCherry), AAV2–DIO–taCasp3–TEVp and AAV2–DIO–hSyn–hm4D(Gi)–mCherry were purchased from the University of North Carolina vector core [first two constructs courtesy of K. Deisseroth (Stanford University), third construct courtesy of N. Shah (University of San Francisco), fourth construct courtesy of B. Roth (University of North Carolina)]. AAV2–ChR2–mCherry expresses an enhanced version of the photosensitive cationic channel ChR2 [ChR2(H134R)] fused to the fluorescent reporter mCherry. In these vectors, the ChR2–mCherry (AAV2–

ChR2–mCherry), mCherry (AAV2–mCherry), taCasp3–TEVp and hm4D(Gi)–mCherry sequences are flanked by the same double lox sites (LoxP and lox 2722).

Injections of viral vector into the rostral ventrolateral medulla (RVLM) and optical fiber placement

AAV2–ChR2–mCherry or AAV2–mCherry was injected unilaterally into the left RVLM; this was followed by placement of an optical fiber. AAV2–DIO–taCasp3–TEVp and AAV2–DIO–hSyn–hm4D(Gi)–mCherry were injected bilaterally into the RVLM; these mice were not instrumented with an optical fiber. The injections were made under aseptic conditions in mice anesthetized with a mixture of ketamine (100 mg/kg) and dexmedetomidine (0.2 mg/kg; ip). Depth of anesthesia was deemed sufficient if the corneal and hind-paw withdrawal reflex were absent. Additional anesthetic was administered as necessary (10% of the original dose, ip). Body temperature was maintained at 37.0 ± 0.5 °C with a servo-controlled temperature pad (TC-1000; CWE). The mandibular branch of the facial nerve was revealed through a small skin incision (left side or both sides as required) for later electrical stimulation. The mice were then placed prone on a Kopf 1730 stereotaxic apparatus adapted for mouse stereotaxic injections (ear bar adaptor, model EB-5N; Narishige Scientific Instrument Lab; bite bar, Model 926 mouse adaptor set at −2 mm; David Kopf Instruments). The viral vector was loaded into a 1.2 mm internal diameter glass pipette broken to a 25 μm tip (external diameter) and introduced into the brain through a 1.5 mm diameter hole that was drilled into the occipital plate caudal to the parieto-occipital suture on the left side (or on both sides). The facial nerve was stimulated (0.1 ms, 1–300 μA, 1 Hz) to evoke antidromic field potentials within the facial motor nucleus[29]. These field potentials, recorded via the vector-filled pipette, were used to map the caudal end of the facial motor nucleus (FN) and thus identify the location of C1 neurons that reside immediately caudal to this nucleus. For unilateral administration of vector, three 140 nL injections were made 300 μm above the base of the medulla oblongata (determined as the lower limit of the facial field potential) and at the medial edge of the respiratory column (identified by respiratory synchronous multiunit activity). The three injections were separated by 200 μm and were aligned rostrocaudally. Next, an optical fiber (125 μm core after desheathing; 0.39 numerical aperture; Thorlabs) was inserted 300 μm above the injection site (fiber tip ~4.7 mm ventral to the dorsal surface of the brain) and then secured to the skull with cyanoacrylate adhesive. Prior to implantation the optical fibers were glued into a zirconia ferrule (outside diameter, 1.25 mm; bore, 130 μm; Precision Fiber Products). The light output of each optical fiber was measured with a light meter (Thorlabs), and the laser setting required to deliver 10 mW was recorded. This setting was later used during the *in vivo* experiments. The stereotaxic procedure used for bilateral injection of AAV2–DIO–taCasp3–TEVp or AAV2–DIO–hSyn–hm4D(Gi)–mCherry into the RVLM was the same except that no optical fiber was inserted.

Mice received postoperative boluses of atipemazole (α_2-adrenergic antagonist, 2 mg/kg, sc), ampicillin (125 mg/kg, ip), and ketoprofen (4 mg/kg, sc). Ampicillin and ketoprofen were readministered 24 h postoperatively. Mice were housed in the University of Virginia vivarium for at least 4 weeks after virus injection. Mice were maintained in groups of 3 – 5 per cage on a 12:12-h light-dark cycle. During this time, mice gained weight normally and

appeared unperturbed by the implanted optical fiber. These mice were randomly divided into the various treatment groups.

Whole body plethysmography

Optogenetic stimulation of C1 cells produces a frequency dependent increase in breathing frequency and amplitude[48]. Breathing patterns evoked by brief periods of C1 cell photostimulation (10 s) were therefore routinely measured in conscious mice to insure that C1 cells were effectively transduced to express ChR2 and that the optical fiber was correctly implanted. Breathing was measured in conscious mice using unrestrained whole-body plethysmography (EMKA Technologies), as described previously[26]. The chamber was continuously flushed with dry room temperature air delivered at 0.5 standardized liters per minute. Fluctuations in chamber pressure were amplified ($\times$ 500) and acquired at 1 kHz with Spike 2 software (v7.06; CED). Respiratory frequency (fR; breaths/min) was measured during periods of behavioral quiescence. The measurements were made between 10:00 am and 4:00 pm. Mice were placed in the plethysmography chamber and habituated to chamber conditions for 2–3 h. At this point, mice were briefly anesthetized with isoflurane while the connection between the implanted fiber optic and the laser was established. Recordings were initiated at least 30 min after the mice had regained consciousness and only during periods of behavioral quiescence. To evaluate the effects of photostimulation on fR, 10-s trains of light pulses (duration, 10 ms) were delivered at various frequencies (5, 10, 15, and 20 Hz). The minority of DBH-cre mice that had received injections of AAV2–ChR2–mCherry and did not have a detectable breathing stimulation at 5 Hz were not included in the experimental group (10 of 182). These mice were used as control group (no laser group in renal ischemia-reperfusion injury (IRI) or corticosterone experiment).

Splenectomy

Mice (DBH-cre; n = 12) were anesthetized with an i.p. injection of ketamine (120 mg/kg) and xylazine (12 mg/kg). Depth of anesthesia was assessed by absence of the corneal and hind-paw withdrawal reflex. Additional anesthetic was administered as necessary (10% of the original dose, ip). Body temperature was maintained at 37.0 ± 0.5 °C with a servo-controlled temperature pad (TC-1000; CWE). A small flank incision was performed through which the splenic vasculature was ligated and the spleen removed. Mice received boluses ketoprofen (4 mg/kg, sc) immediately after surgery and again 24 h later. These mice were allowed to recover for 7 days prior to renal ischemia-reperfusion (IR).

Subdiaphragmatic vagotomy

Subdiaphragmatic vagotomy (sVNX) was performed in 6 DBH-cre mice that had received injections of ChR2-mCherry AAV2 into the RVLM one week prior to testing the effect of C1 cell stimulation on renal IRI. The mice were anesthetized with an i.p. injection of ketamine (120 mg/kg) and xylazine (12 mg/kg). Depth of anesthesia was assessed by absence of the corneal and hind-paw withdrawal reflex. Additional anesthetic was administered as necessary (10% of the original dose, ip). Body temperature was maintained at 37.0 ± 0.5 °C with a servo-controlled temperature pad (TC-1000; CWE). After middle upper laparotomy, the stomach was gently manipulated to expose the esophagus. Then, both anterior and posterior trunks of the vagal nerves were identified between the diaphragm and

the gastric cardia and then transected. In the sham-operated animals (10 DBH-cre mice), the abdominal vagal nerves were similarly exposed but not cut Mice received boluses of ampicillin (125 mg/kg, ip) and ketoprofen (4 mg/kg, sc) immediately after surgery and again 24 h later. Six additional mice (C57BL/6) were used to test the efficacy of the denervation procedure. Three mice were subjected to sVNX and the rest underwent sham surgery, as described above. Seven days after surgery the mice received an i.p. injection of 200 μl of 1% FG. After 4 days, the mice were deeply anesthetized and perfused. Brains were removed and postfixed in 4% paraformaldehyde for up to 3 days, then all brains were sectioned as described below.

Arterial pressure (AP) and heart rate (HR) measurement in conscious mice subjected to C1 cell stimulation or restraint stress

The cardiorespiratory effects (AP, HR, breathing parameters) produced by unilateral optogenetic stimulation of C1 cells were examined in 10 DBH-cre mice prepared as described above. These mice were implanted with a radio-telemetry probe (PA-C10; Data Sciences International) 3 weeks after injection of AAV2–ChR2–mCherry into the RVLM to measure AP (right common carotid artery). A separate cohort of 4 DBH-cre mice was used to measure the effect of 10 min of restraint stress (method described below) on AP and HR; breathing was not measured in these mice. For arterial pressure probe implantation, mice were anesthetized with an i.p. injection of ketamine (120 mg/kg) and xylazine (12 mg/kg) and their body temperature kept at 37.0 ± 0.5 °C. Depth of anesthesia was assessed by absence of the corneal and hind-paw withdrawal reflex. Additional anesthetic was administered as necessary (10% of the original dose, ip). AP and HR were measured a minimum of one week after arterial probe implantation using a PhysioTel Receiver (RLA 1020; Data Science International). Mean AP and HR were calculated from pulsatile AP recordings based on values calibrated before implantation of the telemetry probe. For optogenetic experiments only, the mice were placed in the plethysmography chamber in order to record respiratory parameters along with pulsatile AP. Breathing parameters (fR, Vt, MV) were extracted as described earlier.

In one series of 6 DBH-cre mice we examined the effects of brief (10 s) periods of C1 cell photostimulation delivered at various frequencies (5, 10, 15, and 20 Hz) during behavioral quiescence. This experiment showed that 5 Hz stimulation produces a reliable and submaximal breathing stimulation. On that basis, 5 Hz was selected to examine the effects of longer periods of stimulation on renal IRI (10 min). The effect of 10 min of C1 stimulation at 5 Hz on AP, HR and breathing was examined in 4 DBH-cre mice. The effect of 10 min of restraint stress (restraint method described below) on AP and HR was evaluated in a separate cohort of 4 DBH-cre mice.

Nerve recordings in urethane-anesthetized mice

These experiments on anesthetized mice were designed to examine the consequences of C1 cell optogenetic stimulation on the sympathetic and parasympathetic efferent activities. Vagus nerve activity (VNA) evoked by optogenetic stimulation of C1 cells at various frequencies was recorded in 12 urethane-anesthetized DBH-cre mice (1.6 g/kg urethane i.p. given as a 20% w/v solution). These mice had received injections of AAV2–ChR2–mCherry

4–5 weeks prior and also had an implanted radio-telemetry probe for blood pressure measurement. Depth of anesthesia was assessed by absence of the corneal and hind-paw withdrawal reflex. Additional anesthetic was administered as necessary (10% of the original dose, i.p.). Body temperature was maintained at 37.0 ± 0.5 °C with a servo-controlled temperature pad (TC-1000; CWE). Following induction of anesthesia, the pre-implanted optical fiber was connected to the laser, and mice were placed supine in a stereotaxic frame. A tracheostomy was performed, and mice were mechanically ventilated with pure oxygen (170–220 rpm at 7–8 μL/g; MiniVent type 845; Hugo-Sachs Electronik). In 6 DBH-cre mice we recorded from the left vagus nerve and the left renal sympathetic nerve simultaneously. In the other 6 mice we recorded from the right vagus nerve only (the sympathetic nerve was not recorded). To record VNA, a ~15 mm segment of the cervical vagus nerve (left or right) was dissected free from the carotid artery and the cervical sympathetic chain and the peripheral end of the isolated vagus nerve segment was crushed. The contralateral vagus nerve was always left intact. A renal sympathetic nerve bundle was isolated through a left flank incision. The vagus nerve was placed on a bipolar stainless wire electrode (AS633; Cooner Wire) that was positioned rostral to the crush in order to measure multi-fiber efferent VNA. The renal nerve bundle was placed uncut on identical bipolar stainless-steel electrodes. Electrodes and nerves were then embedded in silicone (Kwik-Sil, WPI). Next, the adequacy of anesthesia was rechecked, and the muscle relaxant agent vecuronium was administered (0.1 mg/kg, i.p.). After this point, the adequacy of the anesthesia was determined by the absence of change in AP and HR in response to a firm hind-paw pinch. Physiological signals were filtered and amplified (AP, 10–1000 Hz, $\times$ 1000; vagus nerve, 30–3000 Hz, $\times$ 10 000; renal nerve: 30–1000 Hz, $\times$ 10 000; BMA-400 amplifier, CWE). The analog signals were digitized (Micro3 1401; CED) and processed using Spike 2 software (v7.06; CED). VNA was high-pass filtered (100 Hz; transition, 50 Hz) when the signal contained a significant electrocardiogram contamination. The final signal processing consisted of half-wave rectification and averaging. AP and HR were recorded as described above. At the end of the experiment, the vagus nerve was cut on the cephalic side of the recording electrode to measure the electrical noise and, if applicable, the ganglionic blocker hexamethonium bromide was administered (30 mg/kg, i.m.) to eliminate renal sympathetic nerve activity (RSNA) and record the portion of the signal representing the electrical noise. The background noise was systematically subtracted and the balance was taken as efferent VNA or RSNA. These multi-fiber recordings are subject to considerable inter-animal variation in amplitude because of differences in electrode configuration, current leak via extracellular fluid and other factors. The effect of trains of C1 cell stimulation (10 s, 5–20 Hz) on VNA and RSNA was therefore normalized by measuring the ratio between the mean nerve activity present while the 10 s stimulus was applied and the resting activity present during the 10 s preceding the stimulus (both values background subtracted). The nerve activity evoked by low frequency stimulation of C1 cells (1 Hz) was determined by constructing peristimulus waveform averages of the half-wave rectified signal (200 sweeps). The amplitude of the peak evoked response was expressed as percent of the pre-stimulus value of the nerve activity after background noise subtraction. Sham C1 photostimulation (Dummy) was done by setting the laser output to 0 mW.

Optogenetic activation of C1 cells and renal IRI

The effect of C1 cell stimulation on renal IRI was examined in DBH-cre mice that had previously received injections of AAV2–ChR2–mCherry or AAV2-mCherry into the left RVLM. These experiments required 90 mice. The breakdown of the various experimental groups and treatments (laser light, drugs, vector) is shown in Supplemental Table 1 for added clarity. All the mice included in the Table were subjected to bilateral renal IRI the day after the treatment indicated in the table. Each experiment also included 12 mice that were not subjected to renal IRI (not shown on the table) in order to ascertain that their creatinine was appropriately low.

Every mouse also carried an implanted optical fiber. Photostimulation of C1 neurons (DBH-cre mice with injections of AAV2-ChR2-mCherry) or sham stimulation (same trains of laser light delivered to DBH-cre mice injected with AAV2-mCherry) was done while the mice were confined to a plethysmography chamber. The mice were placed in one of these chambers for 2 hours, twice a week for 2 weeks in order to habituate them to this environment and thus minimize the associated stress. Laser light produced no effect of any kind (cardiorespiratory, behavior, corticosterone) in DBH-cre mice injected with control vector (ChR2-mCherry), therefore we presume that the light activated C1 cells only when these neurons expressed ChR2.

The mice were briefly anesthetized with isoflurane while the connection between the implanted fiber optic and the laser was established. Drugs were given i.p. thirty min later (30 mg/kg hexamethonium bromide, a ganglionic blocker, n = 6; 30 mg/kg labetalol, a non-selective $\beta_{1/2}$ and $\alpha 1$-adrenergic receptor antagonist, n = 6; 15 mg/kg butoxamine, a selective β_2-adrenergic receptor antagonist, n = 6; or 30 mg/kg mifepristone, a corticosterone receptor antagonist, n = 6). A group of control mice received the volume of vehicle used to dissolve the drugs (0.9% NaCl solution i.p. for all drugs except mifepristone (100% dimethylsulfoxide (DMSO) as control for mifepristone) (n = 6)). Thirty minutes after drug or vehicle administration, light pulses (10 ms duration, 5 Hz) were delivered for 10 min. Control mice, were briefly anesthetized with isoflurane but photostimulation was not applied.

Twenty-four hours after applying the light pulses to the RVLM, mice were anesthetized with an i.p. injection of ketamine (120 mg/kg) and xylazine (12 mg/kg) and bilateral flank incisions were made to access the kidneys. Renal IRI, as previously described[8], was produced by clamping the renal pedicles for exactly 26 minutes in 88 DBH-cre mice. The clamps were then removed and the wound sutured after restoration of blood flow was visually observed. Kidneys were allowed to reperfuse for a period of 24 hours. This surgical procedure was conducted blind, i.e. the person performing the renal clamp had no knowledge of which combination of drug and optogenetic protocol the mice had been subjected to one day earlier. Mice received ketoprofen (4 mg/kg) and ampicillin (125 mg/kg) after surgery. Twenty-four hours after renal ischemia-reperfusion (IR), the mice were euthanized with an overdose of ketamine and xylazine, and the blood (400 – 600 μL) was collected from the orbital sinus. The kidneys were harvested for histology and extraction of RNA for *Kim-1* transcript measurement. Finally, the descending aorta was clamped, the

animal was perfused through the heart with 4% paraformaldehyde and the brain was collected for histology (see sections on renal and brain histology for details).

Effect of 10 min C1 cell stimulation or 10 min renal ischemia on renal *Hif1a* mRNA

These experiments were done in order to determine whether 10 min of C1 cell stimulation in a conscious mouse produces a measurable increase in the renal level of *Hif1a* transcripts indicative of a possibly severe hypoperfusion. The experiments used three groups of mice. Group 1 consisted of unanesthetized DBH-cre mice with AAV2-ChR2-mCherry injections and a preimplanted optical fiber; C1 cells were not stimulated in this group (no light was applied). In a second group of identically prepared DBH-cre unanesthetized mice, C1 cells were optogenetically stimulated for 10 min using our standard parameters (10 ms pulses, 5 Hz). Group 3 mice were anesthetized with an i.p. injection of ketamine (120 mg/kg) and xylazine (12 mg/kg) and subjected to 10 min of complete bilateral renal ischemia. The kidneys were harvested 10 min after cessation of C1 neuron stimulation (group 2) or sham stimulation (group 1, no light applied) or ischemia (group 3). Groups 1 and 2 were anesthetized with an i.p. injection of ketamine (120 mg/kg) and xylazine (12 mg/kg) prior to harvesting the kidneys.

Effect of restraint stress on renal IRI

The effect of restraint stress on renal IRI was also examined in DBH-cre mice. A subset of DBH-cre mice had previously received bilateral microinjections of AAV2–DIO–hSyn–hm4D(Gi)–mCherry (DREADD, n = 12) or AAV2–DIO–taCasp3–TEVp (caspase, n = 12) into the RVLM. A total of 48 mice was required for these experiments. The breakdown of the various experimental groups (mouse strain, vector and drug) is shown in Supplemental Table 2. All the mice shown in the Table were subjected to 26 min renal ischemia followed by 24 hours of reperfusion.

For the DREADD experiments, the receptor agonist clozapine N-oxide (Sigma-Aldrich, 3 mg/kg, n = 6) or its vehicle (saline; n = 6) was injected 30 min before restraint stress. For restraint stress, each mouse was placed in an adequately ventilated 50 ml conical plastic tube (Corning Inc.) for 10 min (n = 36 DBH-cre). They could rotate from a prone to supine position and back again but not turn head to tail. Non-restrained mice were left undisturbed in their home cages (n = 12 DBH-cre). DBH-cre mice with bilateral injections of AAV2–DIO–taCasp3–TEVp were either subjected to restraint stress or left in their home cage.

Twenty-four hours after restraint stress, mice were anesthetized with an i.p. injection of ketamine (120 mg/kg) and xylazine (12 mg/kg) and bilateral renal clamping was performed for 26 min as described in the previous section (n = 48 DBH-cre mice). Mice received ketoprofen (4 mg/kg) and ampicillin (125 mg/kg) after surgery. Twenty-four hours after renal IR, the animals were euthanized with an over dose of ketamine (120 mg/kg) and xylazine (12 mg/kg) and the blood was collected from the orbital sinus for creatinine measurement. Next, we harvested the kidneys for histology and *Kim-1* mRNA measurement, and the mice were perfusion-fixed with paraformaldehyde. Finally the brains were removed for histology.

Effect of C1 cell stimulation or restraint stress on plasma corticosterone

The effect of C1 cell stimulation on plasma corticosterone and related controls was examined in DBH-cre mice that had previously received injections of AAV2–ChR2–mCherry or AAV2-mCherry into the left RVLM. Every mouse also carried an implanted optical fiber. Four weeks after this procedure, the DBH-cre mice that had received injections of AAV2–ChR2–mCherry were placed in a plethysmography chamber and short trains of light pulses (10 s, 5-20 Hz) were applied to ascertain that breathing was stimulated, thereby indicating that C1 cells were properly activated. During the two next weeks, each mouse was habituated to the plethysmography cage for 2 hrs twice a week. The actual experiment was conducted on week seven. Mice were briefly anesthetized with isoflurane while the connection between the implanted fiber optic and the laser delivery system was established, and 10 ms light pulses were delivered for 10 min at 5 Hz. This procedure was carried out in 9 DBH-cre mice. In order to control for the effect of the light itself and for any untoward effect of the vector, we performed two control experiments. For the first control experiment we used 9 DBH-cre mice with AAV2–ChR2–mCherry. Following connection of the optical fiber with the laser and placement of the mice in the customary environment (plethysmography chamber), no light was applied. The second control experiment was done in mice that had been injected with control virus (AAV2–mCherry). These mice (6 DBH-cre) received the same light pulses (5 Hz, 10 ms, 10 min) as the experimental group while in the same environment. All these experiments were conducted between 1 and 5 pm.

For restraint stress, each mouse (DBH-cre) was placed in an adequately ventilated 50 mL conical plastic tube (Corning Inc.) for 10 min. The mice could rotate from a prone to supine position and back again, but not turn head to tail. Six DBH-cre mice were subjected to this treatment. Control mice (6 DBH-cre) were left undisturbed in their home cages. These experiments were also performed between 1 and 5 pm.

Mice were returned to their original cages after restraint stress or delivery of laser light. Sixty minutes later, the mice were quickly anesthetized with isoflurane and blood was immediately collected from the orbital sinus. Plasma corticosterone concentration was subsequently measured with an enzyme-linked immunosorbent assay (Enzo Life Sciences).

Brain histology

Following completion of the in vivo experiments, mice were lethally anesthetized with an overdose of ketamine and xylazine and perfused transcardially with 50 mL of heparinized saline followed by 100 mL of freshly prepared 4% paraformaldehyde in 100 mL sodium phosphate buffer (pH 7.4). Brains were extracted and post-fixed at 4 °C for 24–48 h in the same fixative. Transverse sections (30 μm-thick) were cut on a vibrating microtome and stored in a cryoprotectant solution (20% glycerol plus 30% ethylene glycol in 50 mM phosphate buffer, pH 7.4) at −20 °C.

Immunohistochemical procedures and microscopy were performed as previously described[23]. The following antibodies were used: mCherry protein was detected with anti-DsRed (rabbit polyclonal, 1:500; Clontech #632496; Clontech Laboratories) followed by Cy3-tagged anti-rabbit IgG (1:200, Jackson ImmunoResearch Laboratories); tyrosine

hydroxylase (TH) was detected with a sheep (1:1000, Millipore #AB1542; EMD Millipore) or chicken (1:1000; lot number TH1205; Aves labs) polyclonal antibody followed by Alexafluor488-tagged donkey anti-sheep or Alexafluor488-donkey anti-chicken antibody (1:200; Jackson ImmunoResearch Laboratories). Choline acetyltransferase (ChAT) was detected with a goat polyclonal antibody (1:100, Millipore #AB144P; EMD Millipore) followed by Cy3-tagged donkey anti-goat (1:200; Jackson ImmunoResearch Laboratories).

Brain sections were examined under brightfield and epifluorescence illumination with a Zeiss AxioImager Z.1 microscope equipped with a computer-controlled stage and the Neurolucida software (v10; MBF Bioscience). Cell counts were performed in a 1-in-3 series of sections that were kept in correct sequential order. Sections from different mice were aligned according to their distance from a reference transverse plane identified as 6.48 mm caudal to bregma after Paxinos and Franklin[51]. The plane of this section intersects the caudal most portion of the facial motor nucleus. Images were obtained with a Zeiss MRc camera as TIFF files (1388 × 1040 pixels) and imported into Canvas software (v10; ACD Systems) for the composition of figures. Output levels were adjusted to include all information-containing pixels. Balance and contrast were adjusted to reflect true rendering as much as possible. No other 'photo-retouching' was performed.

Adoptive transfer of splenocytes from stressed to naïve mice

Spleens were harvested from donor mice (WT C57BL/6 mice) 24 hours after restraint stress (10 min). Single-cell suspensions were generated by passing whole spleen through 40-μm filters into PBS. The cell pellet was collected by centrifugation (500 g for 5 minutes) and then treated with red blood cell lysis buffer (BioLegend) for 3 minutes according to the manufacturer's protocol with some modifications. After cell lysis, the samples were centrifuged, the resulting cell pellet was diluted, and 1×10^6, 5×10^6 or 1×10^7 cells were injected into recipient mice (WT C57BL/6 mice) via tail vein 24 hours prior to IR.

Transfer of noradrenaline-preincubated Tcells to naïve mice

CD4+ T cells were isolated from the spleen using the Dynabeads® Untouched™ Mouse CD4 Cells Kit (Thermo Fisher Scientific Inc.) after splenocytes were obtained from unstressed WT C57BL/6 mice (the details of isolating splenocytes are described above). Isolated CD4+ T cells were treated with noradrenaline (Sigma-Aldrich, 10 μM) for 30 minutes at 37° C. After washing the cells with PBS, CD4+ T cells were re-suspended in PBS and 1×10^5 cells (200 μl) were injected into recipient mice (naïve WT C57BL/6 mice) via tail vein 24 hours prior to IR.

Renal histology

The capsule of the harvested kidney was removed. A center transverse section was cut and placed in 4% PLP (4% paraformaldehyde/1.4% DL-lysine/0.2% sodium periodate in 0.1 M sodium phosphate buffer, pH 7.4) for 24 h and then stored in 70% EtOH until paraffin embedding (UVA Research Histology Core). Paraffin sections (5 μm) were cut and stained with hematoxylin and eosin (H&E). The sections were viewed by light microscopy (Zeiss AxioImager Z1/Apotome microscope, Carl Zeiss Microscopy). Photographs were taken with

an AxioCam MRc camera (Zeiss) and brightness/contrast and white balance adjustments were made using StereoInvestigator software (MBF Bioscience).

The extent of acute tubular necrosis was assessed in an unbiased, systematic manner using design-based stereology to achieve statistically accurate random sampling of kidney sections and yielding the percentage of total area of the section occupied by injured tubules as previously described[8]. The investigator was blinded to the experimental identity of the sections. Sections were imaged by using a Zeiss Axio Imager Z1/Apotome Microscope fitted with motorized focus drives and motorized XYZ microscope stage and integrated to a workstation running StereoInvestigator software (MBF Bioscience). The area fraction fractionator probe was used for stereological analysis of the fractional area of the section occupied by tubular necrosis. The following parameters were defined: counting frame, 400×400 μm; sample grid, 800×800 μm; grid spacing, 85 μm. These values were determined empirically such that adequate numbers of sample sites were visited and adequate numbers of markers (indicating injured tubules) were acquired, in keeping with accepted counting rules for stereology. Injured tubules were identified based on the presence of cast formation, tubule dilation, and/or tubular epithelial denucleation. A total of 290 ± 7.6 (mean $\pm$ SEM) grid sites were evaluated per section.

Plasma creatinine measurement

Plasma was prepared by centrifuging heparinized blood at 7000g for 5 minutes. Plasma creatinine (mg/dl) was determined with an enzymatic method with minor modifications from the manufacturer's protocol (twice the volume of sample and standard, and using two-fold serial dilution of the calibrator (standard) provided in the kit; Diazyme Laboratories) that we have validated by using LC-MS[8].

Real-time PCR measurements of *Kim-1, Gapdh* and *Hif(R1α* mRNA in mouse kidneys

Renal mRNA was isolated by following the ethanol-precipitation method, and RNA concentration was determined based on spectrophometric determination of 260/280 ratio. cDNA was generated from the resultant tissue RNA using the iScript cDNA synthesis kit (Bio-Rad, Hercules, CA) as described by the manufacturer. Resultant cDNA was then used to determine relative mRNA expression of Kim-1, Hif-1α, and GAPDH using the iTAC Universal SYBR Green Supermix (Bio-Rad). Primers used were as follows: Kim-1 (fwd) – ACA TAT CGT GGA ATC ACA ACG AC, (rev) – ACT GCT CTT CTG ATA GGT GAC A; GAPDH (fwd) – ACG GCA AAT TCA ACG GCA CAG TCA, (rev) – TGG GGG CAT CGG CAG AAG G. Hif-1α (fwd) – ACC TTC ATC GGA AAC TCC AAA G, (rev) – CTG TTA GGC TGG GAA AAG TTA GG.

Statistical analyses

From our previous study[8], we justified that the sample size is 5 (see check list). All data sets were tested for normality using the D'Agostino & Pearson omnibus normality test or Kolmogorov-Smirnov test, then equal variances were tested using the Brown-Forsythe test. If the criteria of normality and equal variance were satisfied, we evaluated statistical significance using one- or two-way ANOVA followed by the Tukey–Kramer test. When the criteria of normality and equal variance were not met, we used a non-parametric statistical

test (Kruskal-Wallis followed by Steel-Dwass test for multiple comparisons between groups). All values are expressed as means ± SEM and statistical significance is set at $P < 0.05$.

Supplementary Material

Refer to Web version on PubMed Central for supplementary material.

Acknowledgments

References

1. Li L, et al. IL-17 produced by neutrophils regulates IFN-gamma-mediated neutrophil migration in mouse kidney ischemia-reperfusion injury. J Clin Invest. 2010; 120:331–342. [PubMed: 20038794]

2. Pavlov VA, Tracey KJ. Neural circuitry and immunity. Immunol Res. 2015; 63:38–57. [PubMed: 26512000]

3. Olofsson PS, Rosas-Ballina M, Levine YA, Tracey KJ. Rethinking inflammation: neural circuits in the regulation of immunity. Immunol Rev. 2012; 248:188–204. [PubMed: 22725962]

4. Yamakawa K, et al. Electrical vagus nerve stimulation attenuates systemic inflammation and improves survival in a rat heatstroke model. PloS one. 2013; 8:e56728. [PubMed: 23424673]

5. Jiang Y, et al. Vagus nerve stimulation attenuates cerebral ischemia and reperfusion injury via endogenous cholinergic pathway in rat. PloS one. 2014; 9:e102342. [PubMed: 25036185]

6. Katare RG, et al. Differential regulation of TNF receptors by vagal nerve stimulation protects heart against acute ischemic injury. J Mol Cell Cardiol. 2010; 49:234–244. [PubMed: 20302876]

7. Gigliotti JC, et al. Ultrasound Modulates the Splenic Neuroimmune Axis in Attenuating AKI. J Am Soc Nephrol. 2015; 26:2470–2481. [PubMed: 25644106]

8. Inoue T, et al. Vagus nerve stimulation mediates protection from kidney ischemia-reperfusion injury through alpha7nAChR+ splenocytes. J Clin Invest. 2016; 126:1939–52. [PubMed: 27088805]

9. Rosas-Ballina M, et al. Splenic nerve is required for cholinergic antiinflammatory pathway control of TNF in endotoxemia. Proc Natl Acad Sci USA. 2008; 105:11008–11013. [PubMed: 18669662]

10. Reardon C, et al. Lymphocyte-derived ACh regulates local innate but not adaptive immunity. Proc Natl Acad Sci USA. 2013; 110:1410–1415. [PubMed: 23297238]

11. Vida G, et al. beta2-Adrenoreceptors of regulatory lymphocytes are essential for vagal neuromodulation of the innate immune system. FASEB J. 2011; 25:4476–4485. [PubMed: 21840939]

12. Rosas-Ballina M, et al. Acetylcholine-synthesizing T cells relay neural signals in a vagus nerve circuit. Science. 2011; 334:98–101. [PubMed: 21921156]

13. Ueno M, Ueno-Nakamura Y, Niehaus J, Popovich PG, Yoshida Y. Silencing spinal interneurons inhibits immune suppressive autonomic reflexes caused by spinal cord injury. Nat Neurosci. 2016; 19:784–787. [PubMed: 27089020]

14. Martelli D, Yao ST, McKinley MJ, McAllen RM. Reflex control of inflammation by sympathetic nerves, not the vagus. J Physiol(London). 2014; 592:1677–1686. [PubMed: 24421357]

15. Martelli D, McKinley MJ, McAllen RM. The cholinergic anti-inflammatory pathway: A critical review. Auton Neurosci. 2014; 182:65–69. [PubMed: 24411268]

16. Bernik TR, et al. Pharmacological stimulation of the cholinergic antiinflammatory pathway. J Exp Med. 2002; 195:781–788. [PubMed: 11901203]

17. Pavlov VA, et al. Central muscarinic cholinergic regulation of the systemic inflammatory response during endotoxemia. Proc Natl Acad Sci USA. 2006; 103:5219–5223. [PubMed: 16549778]

18. Pullerits R, Oltean S, Floden A, Oltean M. Circulating resistin levels are early and significantly increased in deceased brain dead organ donors, correlate with inflammatory cytokine response and remain unaffected by steroid treatment. J Transl Med. 2015; 13:201. [PubMed: 26112052]

19. Hoeger S, et al. Modulation of brain dead induced inflammation by vagus nerve stimulation. Am J Transplant. 2010; 10:477–489. [PubMed: 20055812]

20. Zhang Y, et al. Autonomic dysreflexia causes chronic immune suppression after spinal cord injury. J Neurosci. 2013; 33:12970–12981. [PubMed: 23926252]

21. Li HY, Ericsson A, Sawchenko PE. Distinct mechanisms underlie activation of hypothalamic neurosecretory neurons and their medullary catecholaminergic afferents in categorically different stress paradigms. Proc Natl Acad Sci USA. 1996; 93:2359–2364. [PubMed: 8637878]

22. Jansen ASP, Nguyen XV, Karpitskiy V, Mettenleiter TC, Loewy AD. Central command neurons of the sympathetic nervous system:basis of the fight-or flight response. Science. 1995; 270:644–646. [PubMed: 7570024]

23. Guyenet PG, et al. C1 neurons: the body's EMTs. Am J Physiol Regul Integr Comp Physiol. 2013; 305:R187–204. [PubMed: 23697799]

24. Dhabhar FS. Effects of stress on immune function: the good, the bad, and the beautiful. Immunol Res. 2014; 58:193–210. [PubMed: 24798553]

25. DePuy SD, et al. Glutamatergic neurotransmission between the C1 neurons and the parasympathetic preganglionic neurons of the dorsal motor nucleus of the vagus. J Neurosci. 2013; 33:1486–1497. [PubMed: 23345223]

26. Abbott SB, Holloway BB, Viar KE, Guyenet PG. Vesicular glutamate transporter 2 is required for the respiratory and parasympathetic activation produced by optogenetic stimulation of catecholaminergic neurons in the rostral ventrolateral medulla of mice in vivo. Eur J Neurosci. 2014; 39:98–106. [PubMed: 24236954]

27. Gigliotti JC, et al. Ultrasound prevents renal ischemia-reperfusion injury by stimulating the splenic cholinergic anti-inflammatory pathway. J Am Soc Nephrol. 2013; 24:1451–1460. [PubMed: 23907510]

28. Wang H, et al. Nicotinic acetylcholine receptor alpha7 subunit is an essential regulator of inflammation. Nature. 2003; 421:384–388. [PubMed: 12508119]

29. Abbott SB, et al. Selective optogenetic activation of rostral ventrolateral medullary catecholaminergic neurons produces cardiorespiratory stimulation in conscious mice. J Neurosci. 2013; 33:3164–3177. [PubMed: 23407970]

30. Stornetta RL, Inglis MA, Viar KE, Guyenet PG. Afferent and efferent connections of C1 cells with spinal cord or hypothalamic projections in mice. Brain Struct Funct. 2016; 221:4027–4044. [PubMed: 26560463]

31. Lee HM, Giguere PM, Roth BL. DREADDs: novel tools for drug discovery and development. Drug Discov Today. 2014; 19:469–473. [PubMed: 24184433]

32. Li YW, Bayliss DA, Guyenet PG. C1 neurons of neonatal rats: intrinsic beating properties and alpha 2-adrenergic receptors. Am J Physiol. 1995; 269:R1356–1369. [PubMed: 8594938]

33. Morgan CW, Julien O, Unger EK, Shah NM, Wells JA. Turning on caspases with genetics and small molecules. Methods Enzymol. 2014; 544:179–213. [PubMed: 24974291]

34. Axelrod J, Reisine TD. Stress hormones: their interaction and regulation. Science. 1984; 224:452–459. [PubMed: 6143403]

35. Ericsson A, Kovacs KJ, Sawchenko PE. A functional anatomical analysis of central pathways subserving the effects of interleukin-1 on stress-related neuroendocrine neurons. J Neurosci. 1994; 14:897–913. [PubMed: 8301368]

36. Miki K, Yoshimoto M. Role of differential changes in sympathetic nerve activity in the preparatory adjustments of cardiovascular functions during freezing behaviour in rats. Exp Physiol. 2010; 95:56–60. [PubMed: 19700516]

37. Oba T, et al. Renal Nerve-Mediated Erythropoietin Release Confers Cardioprotection During Remote Ischemic Preconditioning. Circ J. 2015; 79:1557–1567. [PubMed: 25833080]

38. Bratton BO, et al. Neural regulation of inflammation: no neural connection from the vagus to splenic sympathetic neurons. Exp Physiol. 2012; 97:1180–1185. [PubMed: 22247284]

39. Ninomiya I, Irisawa H. Non-uniformity of the sympathetic nerve activity in response to baroceptor inputs. Brain Res. 1975; 87:313–322. [PubMed: 1092427]

40. Czura CJ, Friedman SG, Tracey KJ. Neural inhibition of inflammation: the cholinergic anti-inflammatory pathway. J Endotoxin Res. 2003; 9:409–413. [PubMed: 14733730]

41. Cano G, Sved AF, Rinaman L, Rabin BS, Card JP. Characterization of the central nervous system innervation of the rat spleen using viral transneuronal tracing. J Comp Neurol. 2001; 439:1–18. [PubMed: 11579378]

42. Chen XH, Itoh M, Sun W, Miki T, Takeuchi Y. Localization of sympathetic and parasympathetic neurons innervating pancreas and spleen in the cat. J Auton Nerv Syst. 1996; 59:12–16. [PubMed: 8816360]

43. Berthoud HR, Powley TL. Characterization of vagal innervation to the rat celiac, suprarenal and mesenteric ganglia. J Auton Nerv Syst. 1993; 42:153–169. [PubMed: 8450174]

44. McAllen RM, May CN, Shafton AD. Functional anatomy of sympathetic premotor cell groups in the medulla. Clin Exp Hypertens. 1995; 17:209–221. [PubMed: 7735270]

45. Burke PG, et al. Optogenetic stimulation of adrenergic C1 neurons causes sleep state-dependent cardiorespiratory stimulation and arousal with sighs in rats. Am J Respir Crit Care Med. 2014; 190:1301–1310. [PubMed: 25325789]

46. Tucker DC, Saper CB, Ruggiero DA, Reis DJ. Organization of central adrenergic pathways: I. Relationships of ventrolateral medullary projections to the hypothalamus and spinal cord. J Comp Neurol. 1987; 259:591–603. [PubMed: 2885348]

47. Schiltz JC, Sawchenko PE. Specificity and generality of the involvement of catecholaminergic afferents in hypothalamic responses to immune insults. J Comp Neurol. 2007; 502:455–467. [PubMed: 17366612]

48. Sun MK, Guyenet PG. Arterial baroreceptor and vagal inputs to sympathoexcitatory neurons in rat medulla. Am J Physiol Reg Integr Physiol. 1987; 252:R699–R709.

49. Zhao YX, et al. Transcutaneous auricular vagus nerve stimulation protects endotoxemic rat from lipopolysaccharide-induced inflammation. Evid Based Complement Alternat Med. 2012; 2012:627023. [PubMed: 23346208]

50. Lim HD, Kim MH, Lee CY, Namgung U. Anti-Inflammatory Effects of Acupuncture Stimulation via the Vagus Nerve. PloS one. 2016; 11:e0151882. [PubMed: 26991319]

51. Paxinos, G., Franklin, KBJ. The Mouse Brain in Stereotaxic Coordinates. Academic Press; New York: 2013.

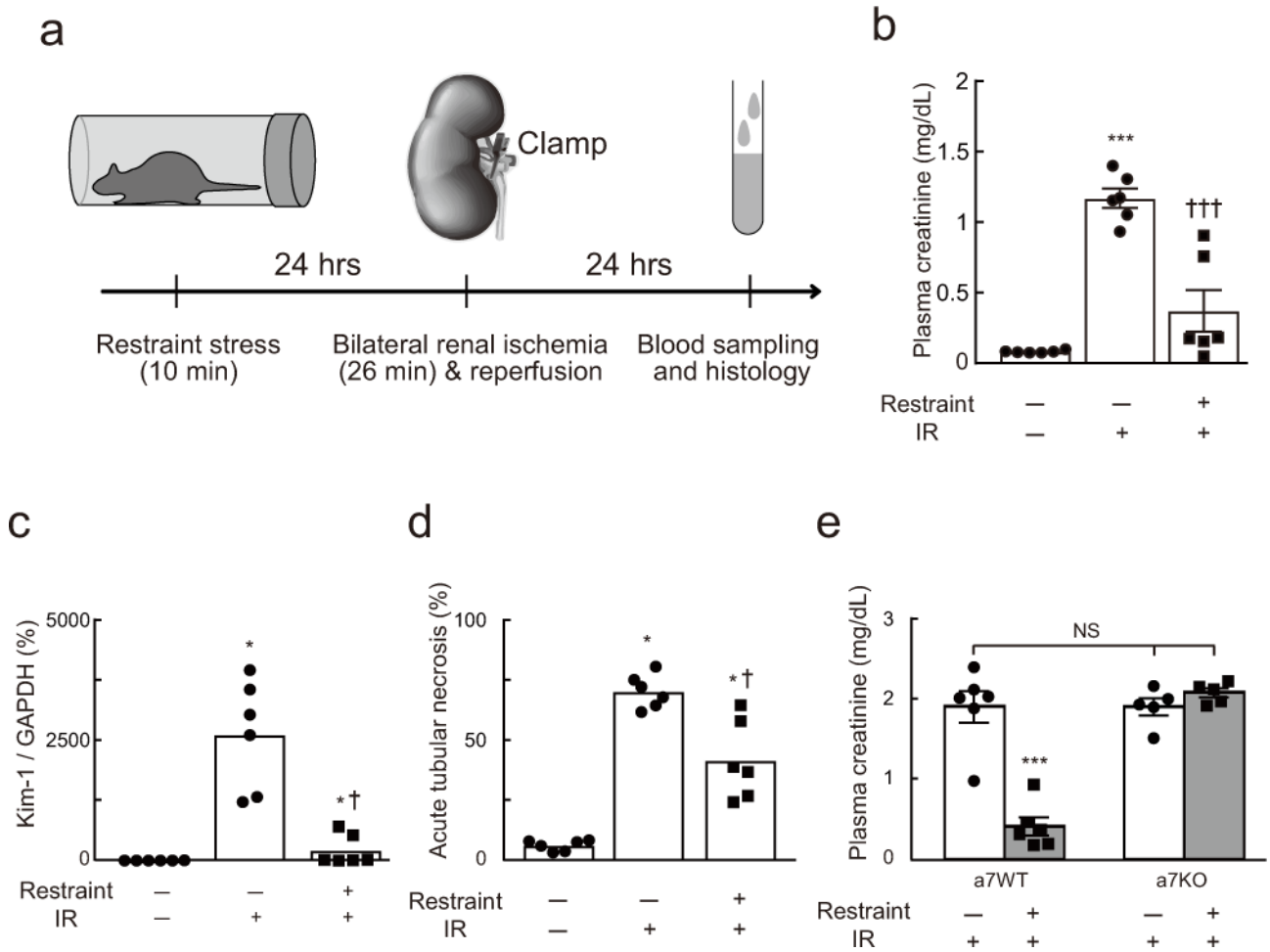**Figure 1. Restraint stress protects against renal ischemia-reperfusion injury (IRI)**
(a) Time line of experiments shown in panels b-e. Effect of prior restraint stress on plasma creatinine in DβH^Cre/0 (dopamine β-hydroxylase) mice (DBH-cre mice) (b), Kidney Injury Molecule-1 (Kim-1) mRNA (DBH-cre mice) (c), and acute tubular necrosis (DBH-cre mice) (d) (n = 6/group). IR, ischemia-reperfusion. One-way ANOVA with Tukey–Kramer test (b) or Kruskal-Wallis with Steel-Dwass test (c and d) was used for statistical analysis; [$F_{(2, 15)}$ = 35.64, $P < 0.0001$] (b), [H = 14.36, $P < 0.0001$] (c), and [H = 14.36, $P < 0.0001$] (d). * vs. Restraint(−):IR(−); † vs. Restraint(−):IR(+). Single or triple significant symbols indicate $P < 0.05$ or $P < 0.001$, respectively. (e) Restraint stress protects wild-type mice (α7WT) against IRI but has no effect in *α7nAChR*^−/− mice (α7KO). Statistics: two-way ANOVA with Tukey–Kramer test; [$F_{(1, 18)}$ = 37.03, $P < 0.0001$]. *** $P < 0.001$ vs. Restraint(−):IR(+) in α7WT and α7KO or Restraint(+):IR(+) in α7KO.
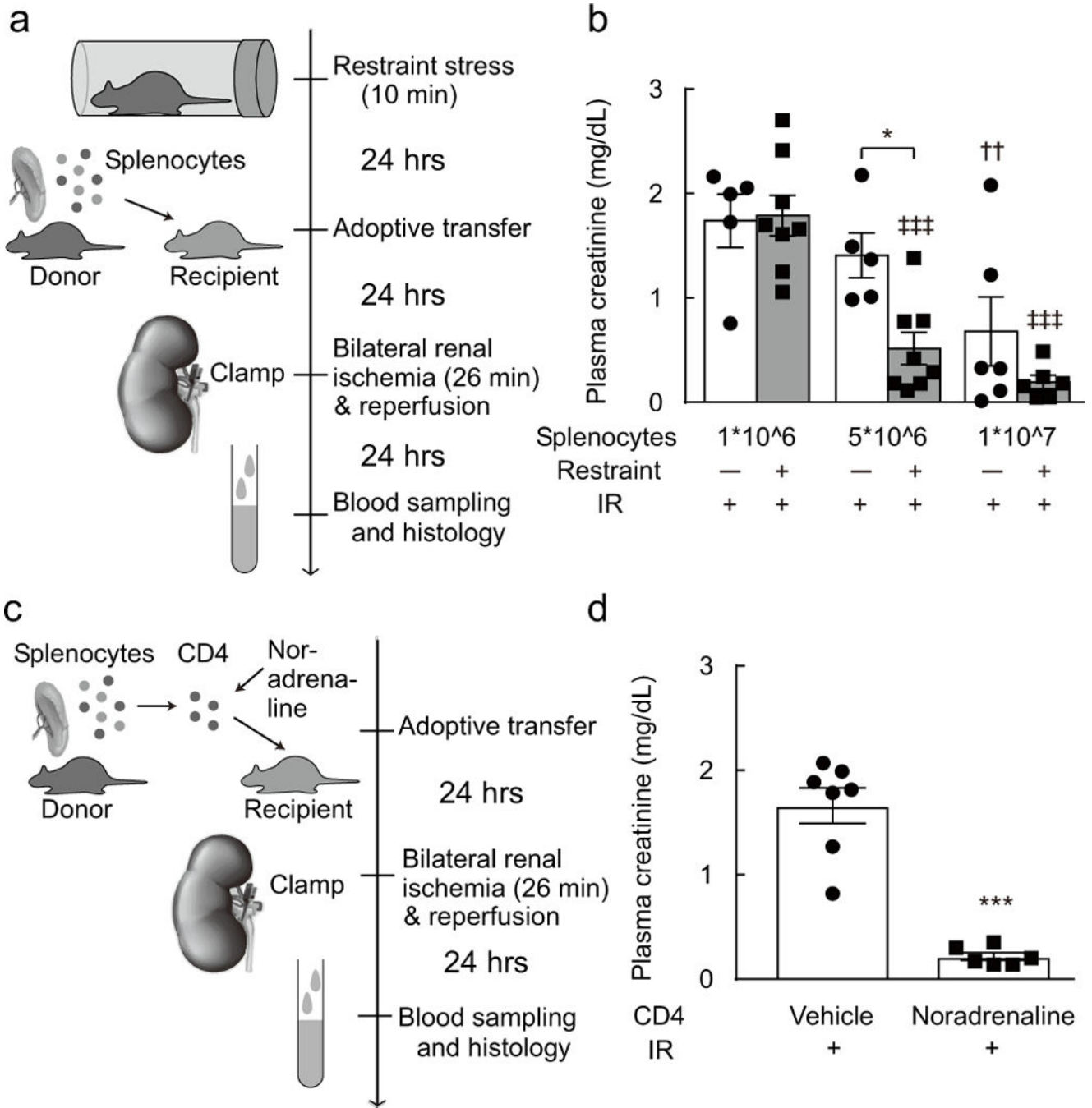
Figure 2. Adoptive transfer of splenocytes protects against renal IRI

(a, b) adoptive transfer of splenocytes. Splenocytes were harvested from restraint stress-exposed donor mice. Then these cells (1*10^6, 5*10^6, or 1*10^7) were injected to the recipient mice. Statistics: two-way ANOVA with Tukey–Kramer test; [$F(1, 32) = 6.299$, $P < 0.0173$]. * $P < 0.05$ vs. 5*10^6:Restraint(−):IR(+), †† $P < 0.01$ vs. 1*10^6:Restraint(−):IR(+), and ‡‡‡ $P < 0.001$ vs. 1*10^6:Restraint(+):IR(+). (c, d) adoptive transfer of noradrenaline-treated CD4 T cells. CD4 T cells were harvested from splenocytes of the donor mice, these cells were treated with noradrenaline. Then these cells were

injected to the recipient mice. Statistics: unpaired t test; [t(11) = 7.657, P < 0.0001]. *** P < 0.001 vs. vehicle.
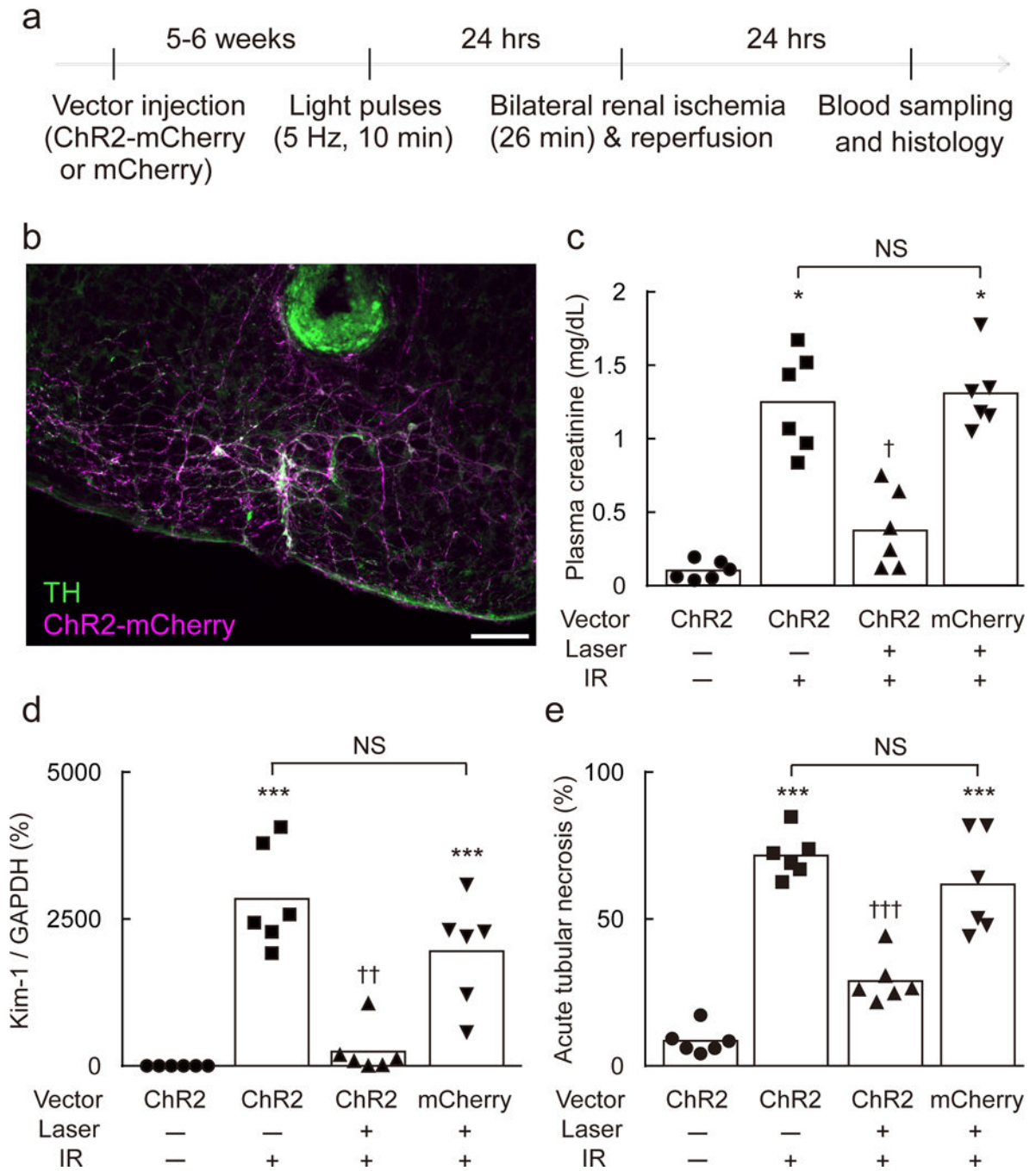
Figure 3. C1 neuron stimulation protects against renal IRI

(a) Time line of experiment. (b) Section through the rostral medulla oblongata of a DBH-cre mouse 5–6 weeks after local injection of AAV2–DIO–EF1α–ChR2–mCherry. mCherry (magenta) and tyrosine-hydroxylase (TH, green) immunoreactivities are colocalized (white). Most catecholaminergic neurons contain mCherry. A small lesion surrounded by green autofluorescence shows the location of the tip of the optical fiber (scale bar: 100 μm). (c–e) Effect of prior C1 neuron stimulation on plasma creatinine, Kidney Injury Molecule-1 (Kim-1) mRNA (*Havcr1/Gapdh* ratio) in the kidney, and acute tubular necrosis (% of kidney

section surface area) in DBH-cre mice after IRI (n = 6/group). Vector used: AAV2–DIO–EF1α–ChR2–mCherry (ChR2) or AAV2–DIO–EF1α–mCherry (mCherry). Laser: 5 Hz, 10 min. IR, ischemia-reperfusion. Statistical analysis (Kruskal-Wallis with Steel-Dwass test): [$H = 18.62$, $P = 0.0003$] (c), [$H = 19.22$, $P = 0.0004$] (d), [$H = 19.77$, $P < 0.0001$] (e), * vs. ChR2:Laser(−):IR(−); † vs. ChR2:Laser(−):IR(+) or mCherry:Laser(+):IR(+). Single, double, or triple significant symbols indicate $P < 0.05$, $P < 0.01$, or $P < 0.001$, respectively.

Figure 4. C1 neurons mediate the protective effect of restraint stress against renal ischemia-reperfusion injury (IRI)

(a) mCherry (magenta) and TH (green) immunoreactivity in the left medulla oblongata of a DBH-cre mouse six weeks after stereotaxic microinjection of AAV2–DIO–hSyn–hm4D(Gi)–mCherry (DREADD) (transverse section; scale bar: 100 μm). (b) Rostrocaudal distribution (mm caudal to bregma) of mCherry and TH immunoreactivities (n = 12). (c) Choline acetyltransferase- (ChAT; magenta) and TH- (green) immunoreactivities in the left medulla oblongata of a DBH-cre mouse 6 weeks after injection of AAV2–DIO–taCasp3–TEVp (AAV2-caspase). After AAV2-caspase treatment, the C1 neurons in the rostral

ventrolateral medulla (RVLM) are undetectable (left and lower middle panels) but other catecholaminergic neurons (dorsal medulla, DMM and locus coeruleus, LC) are intact (top middle and top right panels). ChAT+ neurons are unaffected by AAV2-caspase treatment regardless of location (left and bottom middle). Scale bar: 500 μm (left) or 100 μm (four right panels). Amb, nucleus ambiguus. (d) Rostrocaudal distribution of TH-immunoreactive RVLM neurons in control DBH-cre mice (n = 7) vs. caspase-treated DBH-cre mice (n = 10). Lesions were bilateral; cells were counted on one side only. Statistics: two-way ANOVA with Tukey–Kramer test; [$F_{(12, 180)}$ = 25.99, $P < 0.0001$]. (e) The protective effect of restraint stress against renal IRI was attenuated by inhibiting (DREADD) or lesioning (caspase) the C1 neurons (n = 6 DBH-cre mice/group). CNO: clozapine N-oxide (3 mg/kg); Vehicle: saline. Statistics: one-way ANOVA with Tukey–Kramer test; [$F_{(5, 30)}$ = 14.11, $P < 0.0001$]. * vs. Restraint(-):IR(+) and † vs. Restraint(+):IR(+) and DREADD:Vehicle:Restraint(+):IR(+). Single, double, or triple significant symbols indicate $P < 0.05$, $P < 0.01$, or $P < 0.001$, respectively.
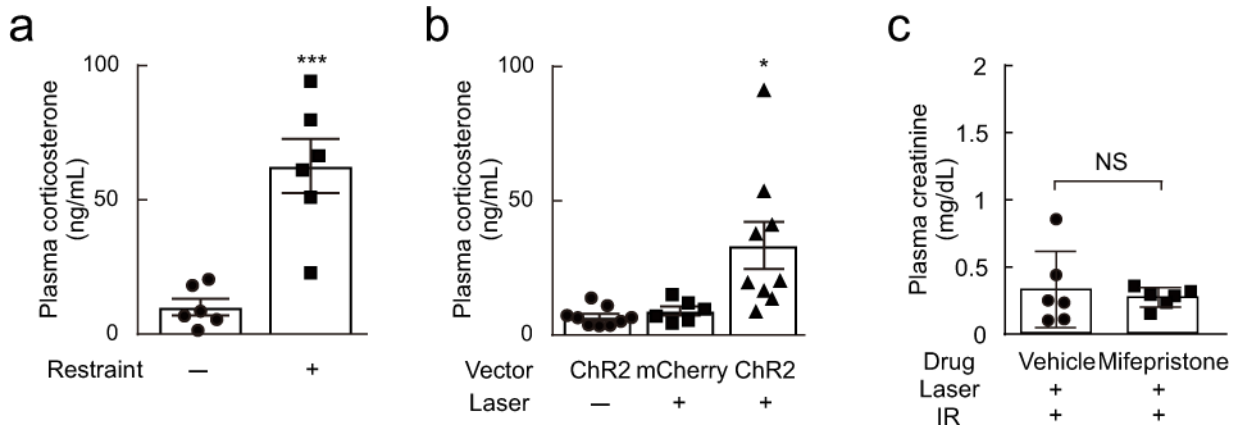
Figure 5. Corticosterone is released by C1 stimulation and restraint stress but plays no detectable role in protecting kidneys from renal ischemia-reperfusion injury (IRI)
(a) Restraint stress increased plasma corticosterone in DBH-cre mice. Statistics: unpaired t test; [$t(10) = 4.991$, $P = 0.0005$]. *** $P < 0.001$ vs. Restraint(−). (b) C1 neuron optogenetic stimulation (AAV2–DIO–EF1α–ChR2–mCherry, ChR2) increased plasma corticosterone in DBH-cre mice whereas laser light alone was ineffective in DBH-cre mice injected with control vector (AAV2–DIO–EF1α–mCherry, mCherry). Laser: laser stimulation (5 Hz for 10 min). Statistics: one-way ANOVA with Tukey–Kramer test; [$F(2, 21) = 6.959$, $P = 0.0048$]. * $P < 0.05$ vs. ChR2:Laser(−) and mCherry:Laser(+). (c) Mifepristone (30 mg/kg) did not alter the protective effect of C1 neuron stimulation against renal IRI in DBH-cre mice (n = 6/group). Statistics: unpaired t test; t(10) = 0.495, $P = 0.6313$).
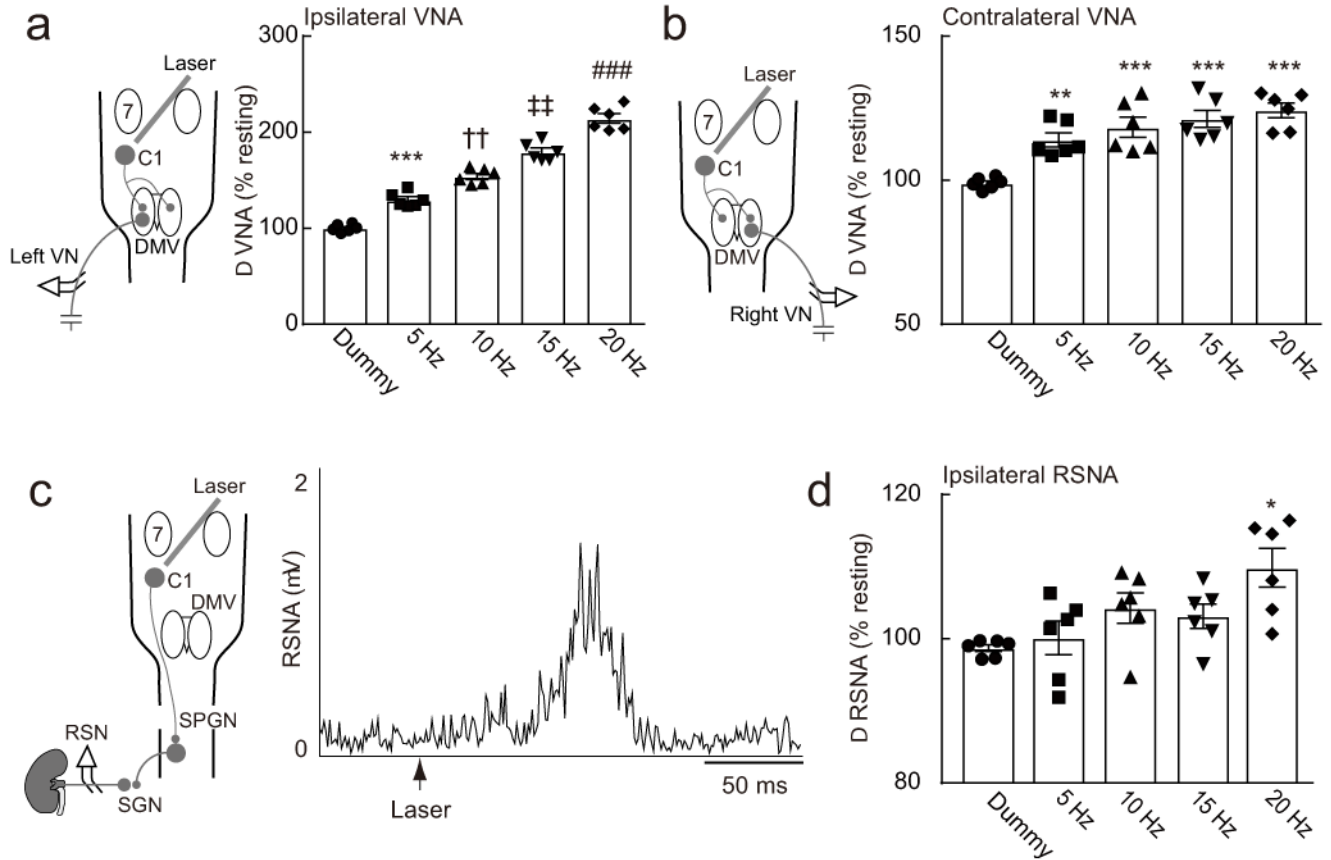
Figure 6. C1 neuron stimulation activates both divisions of the autonomic nervous system
(a) C1 stimulation (left side; 10 ms pulses, 10 s trains) activates ipsilateral vagal nerve efferent activity (VNA) in DBH-cre mice. (b) C1 stimulation (left side; 10 ms pulses, 10 s trains) activates contralateral vagal nerve efferent activity (VNA) in DBH-cre mice. Statistics: repeated measure one-way ANOVA with Tukey–Kramer test; $[F_{(4, 25)} = 112.9, P < 0.0001]$ (a) and $[F_{(4, 25)} = 14.4, P < 0.0001]$ (b). * vs. Dummy, † vs. Dummy and 5 Hz, ‡ vs. Dummy, 5 Hz, and 10 Hz, and # vs. Dummy, 5 Hz, 10 Hz, and 15 Hz. Double symbols, $P < 0.01$; triple symbols, $P < 0.001$. (c) C1 neuron stimulation (10 ms, 1 Hz) produced a robust activation of renal sympathetic nerve activity (RSNA) in DBH-cre mice. (d) Effect of repetitive C1 stimulation (5-20 Hz; 10 ms pulses, 10 s train) on RSNA. Statistics: repeated measure one-way ANOVA with Tukey–Kramer test; $[F_{(4, 25)} = 4.651, P = 0.0061]$. * $P < 0.05$ vs. Dummy and 5 Hz. DMV, dorsal motor nucleus of the vagus; RSN, renal sympathetic nerve; SGN, sympathetic ganglionic neuron; SPGN, sympathetic preganglionic neurons; 7, facial motor nucleus.
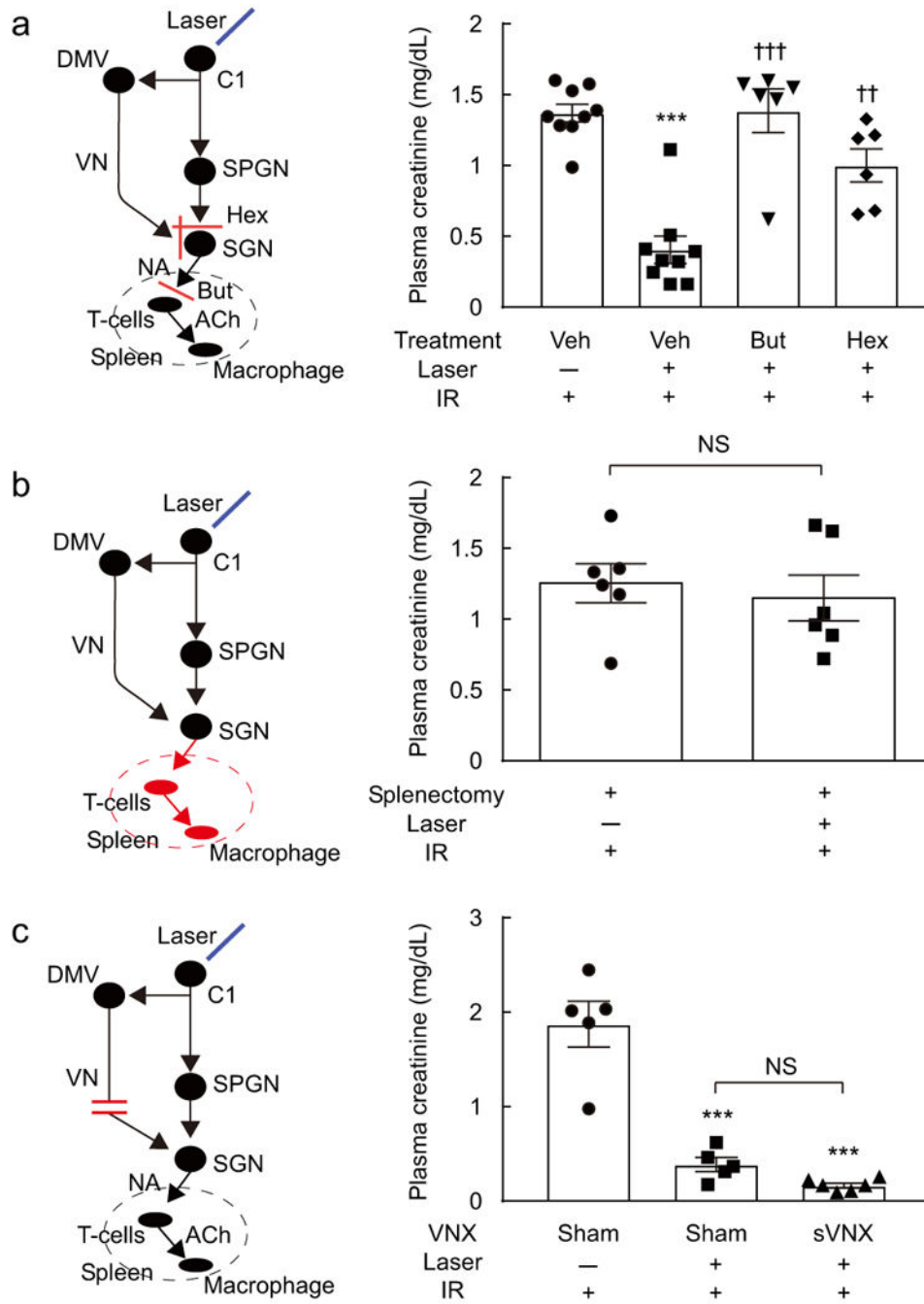
Figure 7. Protection against renal IRI by C1 neuron stimulation is mediated via the autonomic nervous system and the spleen

(a) Butoxamine (But), or hexamethonium (Hex) but not vehicle (Veh) attenuated the protective effect of C1 neuron stimulation (Laser 5 Hz, 10 min) against ischemia-reperfusion (IR) injury (n = 6 or 9 DBH-cre mice/group). Statistics: one-way ANOVA with Tukey–Kramer test; $[F(3, 26) = 22.17, P < 0.0001]$. * vs. Veh:Laser(−):IR(+), † vs. Veh:Laser(+):IR(+). Double symbols, $P<0.01$; triple symbols, $P < 0.001$. (b) Splenectomy eliminated the protective effect of C1 neuron stimulation in DBH-cre mice (n = 6/group). Statistics: unpaired t test; t(10) = 0.49, $P = 0.63$. (c) Subdiaphragmatic vagotomy (sVNX)

does not reduce the protective effect of C1 neuron stimulation in DBH-cre mice (n = 6/group). Statistics: one-way ANOVA with Tukey–Kramer test; [$F_{(2, 13)}$ = 44.75, $P <$ 0.0001]. * vs. Sham:Laser(−):IR(+). Triple symbols, $P < 0.001$. DMV, dorsal motor nucleus of the vagus; NA, noradrenaline; ACh, acetylcholine; SGN, sympathetic ganglionic neuron; SPGN, sympathetic preganglionic neurons; VN, vagal nerve.
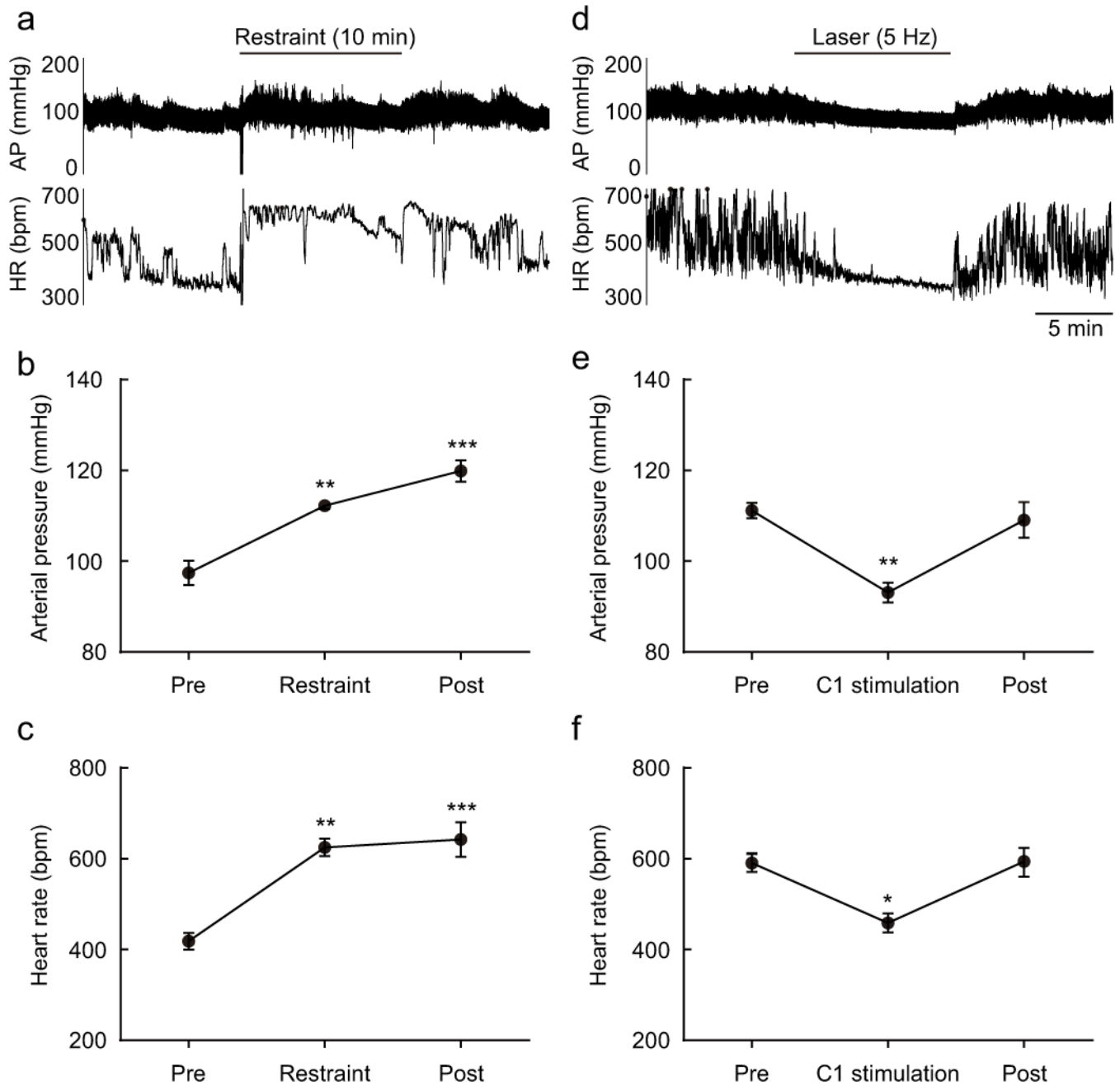
Figure 8. Restraint stress and C1 neuron stimulation produce opposite effects on arterial pressure and heart rate

(a) Effect of restraint stress on arterial pressure (AP) and heart rate (HR) in a DBH-cre mouse. (b and c) Mean AP and HR before (Pre), during and after (Post) restraint (each period: 10 min) in DBH-cre mice (n = 4). Statistics: one-way repeated measures ANOVA with Tukey–Kramer test; [$F_{(2, 9)}$ = 29.11, P = 0.0001] (b) and [$F_{(2, 9)}$ = 21.93, P = 0.0003] (c). * vs. Pre. Double symbols, P < 0.01 and triple symbols, P < 0.001. (d) Effect of C1 stimulation (10 ms, 5 Hz, 10 min) on arterial pressure (AP) and heart rate (HR) in a DBH-cre mouse. (e and f) Effect of C1 neuron stimulation (laser 5 Hz) on AP and HR in DBH-cre mice. Mean AP and HR before (Pre), during and after (Post) C1 neuron stimulation (each

period: 10 min) (n = 4/group). Statistics: one-way repeated measure ANOVA with Tukey–Kramer test; $[F_{(2, 9)} = 12.7, P = 0.0024]$ (e) and $[F_{(2, 9)} = 9.249, P = 0.0066]$ (f). * vs. Pre. Single symbols, $P < 0.05$ and double symbols, $P < 0.01$.